Uses of SYNOPSYS in High-Energy Physics experiments

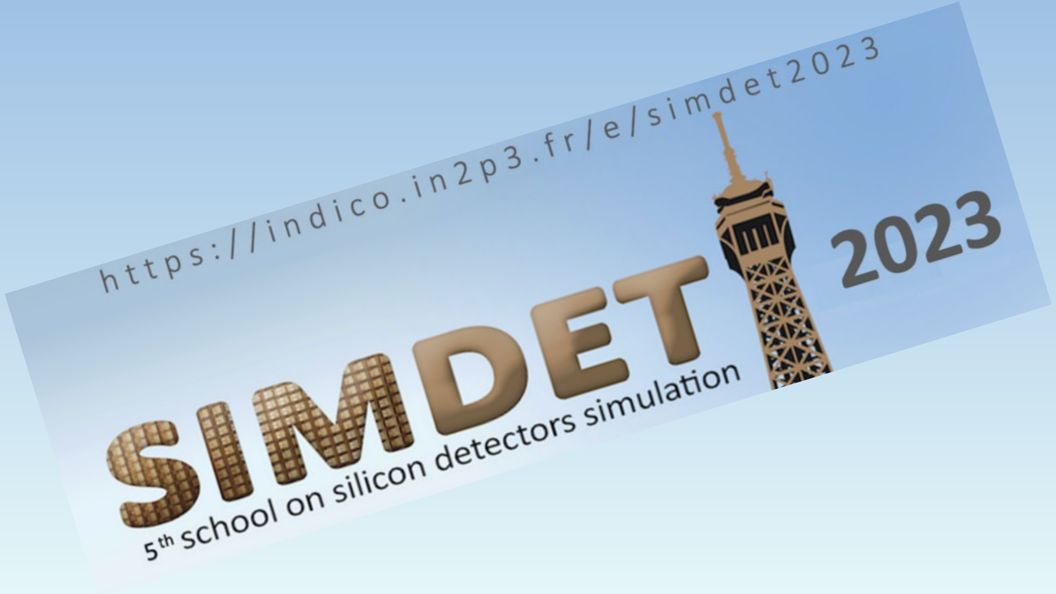

A. Morozzi
INFN Perugia

Outline

- Layout development
  - Process simulations
  - Sentaurus Structure Editor approach
- Device-level & Mixed mode simulations
  - Rad-hard devices
  - Rad-Hard and innovative materials
  - Radiation damage effects models
- Combine TCAD and AllPix Squared
- Conclusions

❗ Selective, non-complete set of examples from HEP experiments

Motivations and Challenges

- ❑ Performance of complex sensors is not analytically predictable anymore!
  → Increasing need for TCAD simulations.
- ❑ Semiconductor detectors will face increasing radiation levels
  - ▪ $>1\text{x}10^{16}$ 1MeV n_{eq}/cm^2 (HL-LHC);
  - ▪ $>5\text{x}10^{17}$ 1MeV n_{eq}/cm^2 (FCC-hh);
    - ▪ detectors used at LHC cannot be operated after such irradiation.

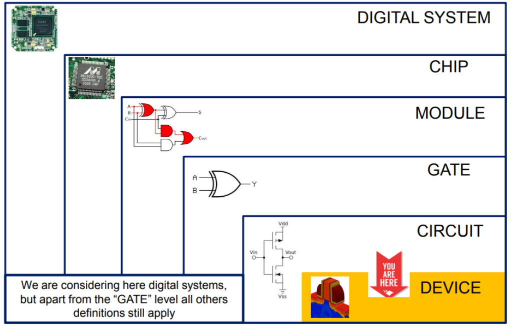

We are considering here digital systems, but apart from the "GATE" level all others definitions still apply

- ❑ New requirements lead to new detector technologies
  - ▪ Need to be optimized for radiation hardness and/or 4D tracking capabilities.
- ❑ Modern TCAD simulation tools can have a crucial role in radiation-hard device design
  - ❑ Reducing costly and time-consuming physical testing.
  - ❑ To get insights. Deep understanding of physical device behavior.
  - ❑ To quickly screen technological options and drive the industrial strategy.
  - ❑ Combined Bulk and surface radiation damage can be considered.
  - ❑ Within a hierarchical approach, increasingly complex models can be considered, by balancing complexity and comprehensiveness.

arianna.morozzi@pg.infn.it

The Technology-CAD modeling approach

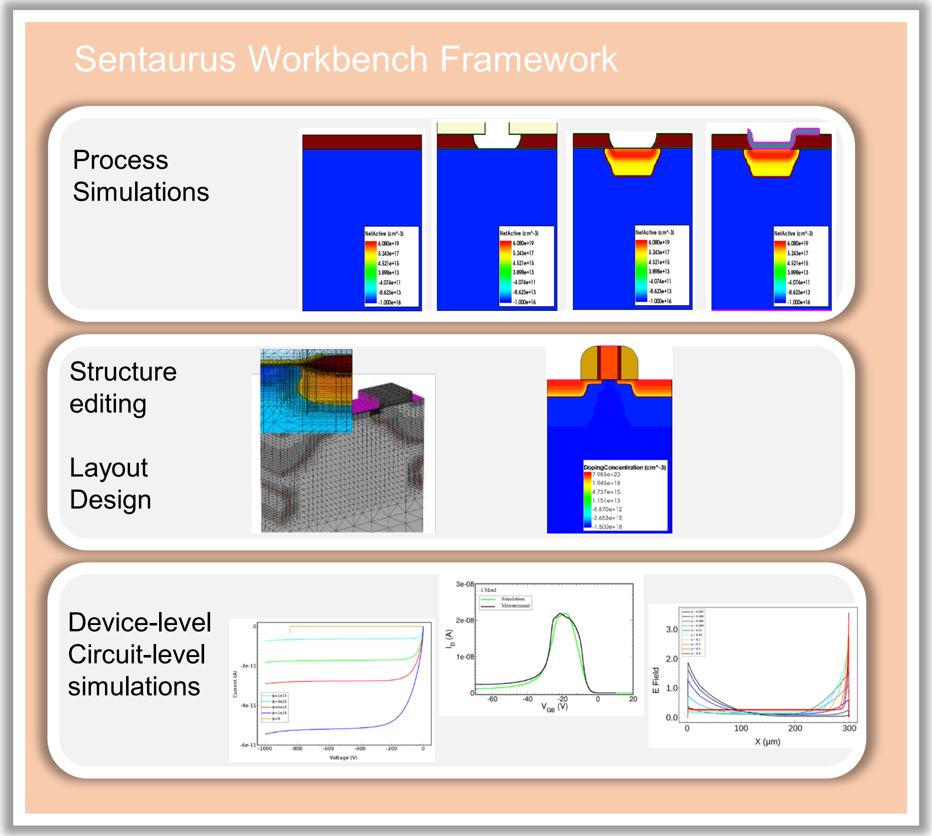

- √ TCAD simulation tools solve fundamental, physical partial differential equations, such as diffusion and transport equations for discretized geometries (finite element meshing).
- √ This deep physical approach gives TCAD simulation predictive accuracy.
- ✓ Synopsys© Sentaurus TCAD

$$\left\{\begin{array}{ll} \nabla\cdot(-\varepsilon_s\nabla\varphi)=q\left(N_D^+-N_A^-+p-n\right) & \text{Poisson} \\ \dfrac{\partial n}{\partial t}-\dfrac{1}{q}\nabla\cdot\vec{J}_n=G-R & \text{Electron continuity} \\ \dfrac{\partial p}{\partial t}+\dfrac{1}{q}\nabla\cdot\vec{J}_p=G-R & \text{Hole continuity} \end{array}\right.$$

$$\vec{J}_n=-q\mu_n n\nabla\varphi+qD_n\nabla n$$

$$\vec{J}_p=-q\mu_p p\nabla\varphi-qD_p\nabla p$$

arianna.morozzi@pg.infn.it

Process simulations

Synopsys Sentaurus TCAD Sprocess simulations
for HEP experiments

Process simulations for HEP

- Sprocess: powerful tool for emulating the technological steps of a fabrication process

- Why process simulation in HEP?
  - Doping profiles are critical for e.g., breakdown etc
  - Increasing relevance in HEP due to advanced sensor processes needed to reach ambitious requirements of future silicon detectors in HEP

- Aim: Investigate new technology process options/Optimize doping profiles
  - Simulate doping profiles obtained by specific processing techniques, calibrate the model with experimental data, and then optimize the process to obtain the desired profile/performance.
  - It requires detailed modeling of the process of manufacturing.
  - Calibration of models needs expensive experiments physical-chemical investigations).
    —> Close collaboration with foundries (e.g., ad-hoc wafer fabrication, SIMS measurements, …).

Often the process details are not known to us
➞ Start with analytical doping profiles based on best guesses in Sentaurus Structure Editor

arianna.morozzi@pg.infn.it

sprocess simulation

- MOSFET modeling
- Modeling of semiconductor-chip process-manufacturing steps like lithography, deposition, etching, ion implantation, diffusion, oxidation, silicidation, mechanical stress, etc

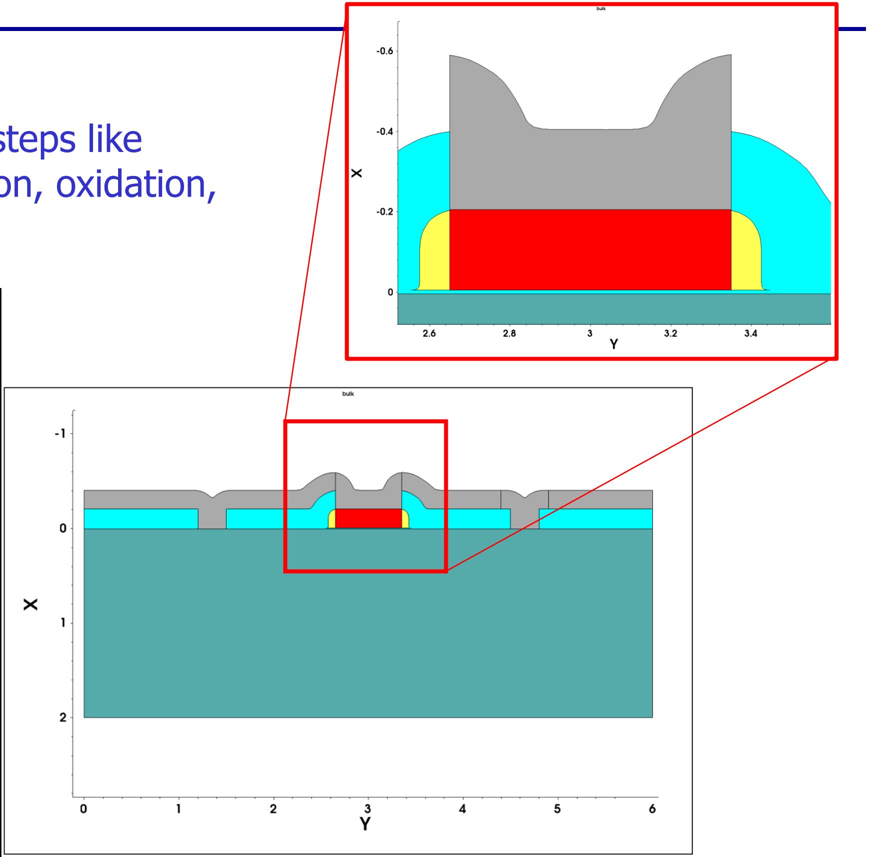

arianna.morozzi@pg.infn.it

Sde simulations

Synopsys Sentaurus TCAD Sde simulations
for HEP experiments

arianna.morozzi@pg.infn.it

Low Gain Avalanche Diodes

This work has been supported by the Italian PRIN MIUR 2017 "4DInSiDe" under GA No 2017L2XKTJ, by the European Union's Horizon 2020 Research and Innovation programme under GA No 101004761 "eXFlu-innova" and it has been conducted in collaboration with the INFN CSN5 "eXFlu" research project.

- **Low-Gain Avalanche Diode (LGAD)**
  - **n-in-p silicon** sensors
  - Operated in **low-gain regime** (20 – 30)
  - **Critical electric field ~ 20 – 30 V/µm**
  - Good candidates for **4D tracking**
  - Mitigation of the radiation damage effects by exploiting the **controlled charge multiplication** mechanism.

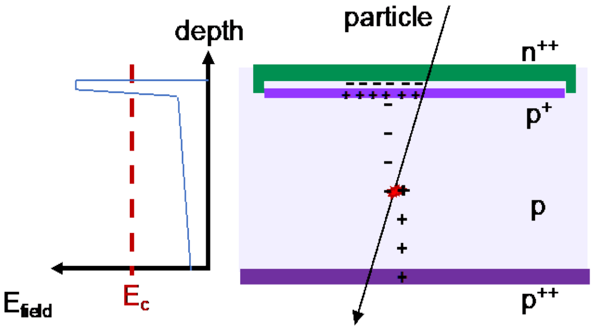

- **Advanced TCAD** modeling
  - **Radiation damage effects** model implementation
  - Accounts for the acceptor removal mechanism[5] which deactivates the p+-doping of the gain layer with irradiation.
  - Electrical behavior **prediction/ performance optimization** up to the highest fluences.

Layout and **doping profile**

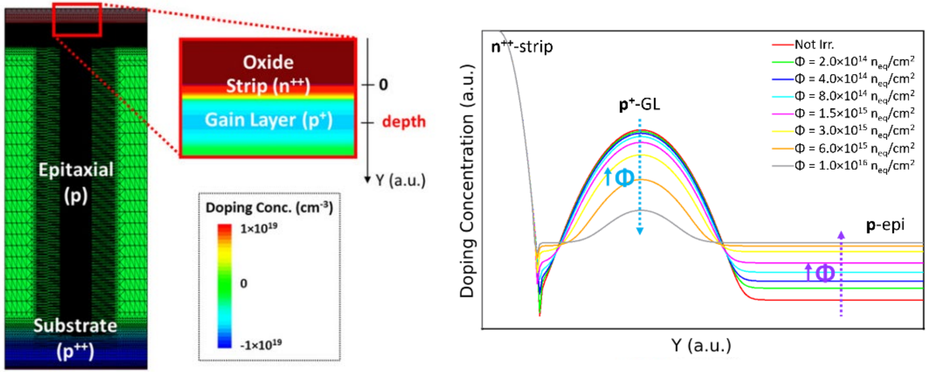

M. Ferrero et al., doi:10.1016/j.nima.2018.11.121
T. Croci et al 2022 JINST 17 C01022

arianna.morozzi@pg.infn.it

Gain layer sensitivity analysis

This work has been supported by the Italian PRIN MIUR 2017 "4DInSiDe" under GA No 2017L2XKTJ, by the European Union's Horizon 2020 Research and Innovation programme under GA No 101004761 "eXFlu-innova" and it has been conducted in collaboration with the INFN CSN5 "eXFlu" research project.

- Three different doping profiles considered
  - Shallow, Standard, Deep.
  - **Gain layer** peak:
    a variation of a few percentages affects the breakdown voltage (V_{BD}).
  - Effect on the gain layer depletion voltage.
  - **Predictive** analysis on sensor performance considering the **radiation damage effects**.

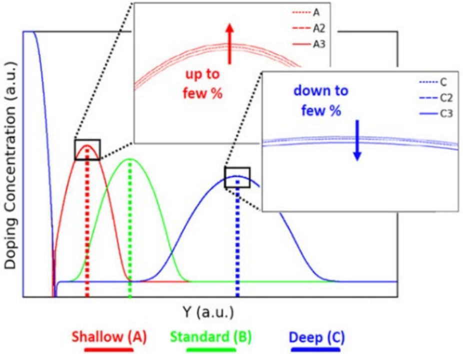

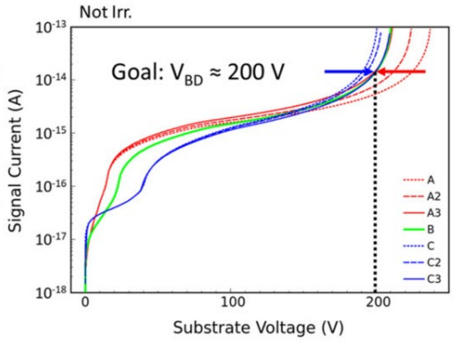

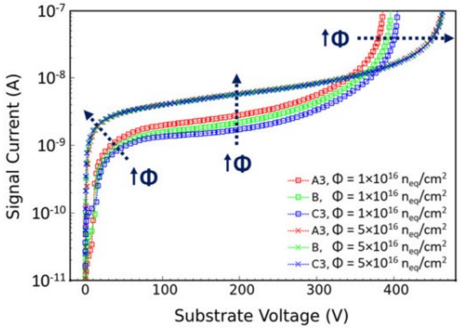

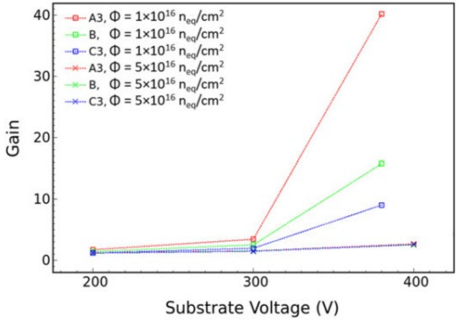

T. Croci et al 2023 JINST 18 C01008.

Device and Mixed-mode simulations

Synopsys Sentaurus TCAD Sdevice simulations
for HEP experiments

arianna.morozzi@pg.infn.it

TCAD simulation of LGAD devices

✓ **Physical models**

- **Generation/Recombination rate**
  - Shockley-Read-Hall, Band-To-Band Tunneling, Auger
  - **Avalanche Generation => impact ionization models,** *van Overstraeten-de Man, Okuto-Crowell, Massey*[1], *UniBo*
- **Fermi-Dirac statistics**
- **Carriers mobility variation** doping and field-dependent
- **Physical parameters**
  - e-/h+ recombination lifetime

✓ **Radiation damage models: "PerugiaModDoping"**

- **"New University of Perugia model"**
  - **Combined surface and bulk** TCAD damage modeling scheme[2]
  - Traps generation mechanism
- **Acceptor removal mechanism** => $N_{GL}(\phi) = N_A(0)e^{-c\phi}$
  - where
    - **Gain Layer** (**GL**), **c** removal rate (**Torino parameterization**[3])
- **Acceptor creation**

$$N_{A,bulk} = \begin{cases} N_{A,bulk}(0) + g_c\phi, & 0 < \phi < 3E15\ n_{eq}/cm^2 \\ 4.17E13 \cdot \ln(\phi) - 1.41E15, & \phi > 3E15\ n_{eq}/cm^2 \end{cases}$$

where g_c = 0.0237 cm^{-1} (**Torino acceptor creation**)

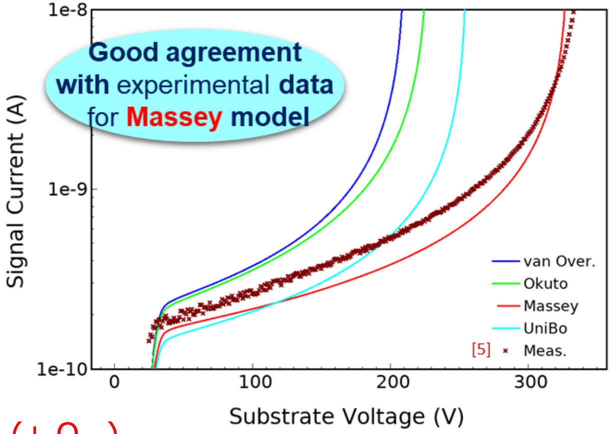

Good agreement with experimental **data** for **Massey model**

Surface damage (+ Q_{OX})

Type	Energy (eV)	Band width (eV)	Conc. (cm^{-2})
Acceptor	$E_C \le E_T \le E_C$-0.56	0.56	$D_{IT} = D_{IT}(\Phi)$
Donor	$E_V \le E_T \le E_V$+0.6	0.60	$D_{IT} = D_{IT}(\Phi)$

Bulk damage

Type	Energy (eV)	η (cm^{-1})	σ_n (cm^2)	σ_h (cm^2)
Donor	E_C - 0.23	0.006	2.3×10^{-14}	2.3×10^{-15}
Acceptor	E_C - 0.42	1.6	1×10^{-15}	1×10^{-14}
Acceptor	E_C - 0.46	0.9	7×10^{-14}	7×10^{-13}

[1] M. Mandurrino et al., IEEE NSSMIC 2017.
[2] D. Passeri, AIDA2020 report, CERN Document Server.
[3] M. Ferrero et al., https://doi.org/ 10.1016/j.nima.2018.11.121.
[4] V. Sola et al., https://doi.org/10.1016/j.nima.2018.07.060.

arianna.morozzi@pg.infn.it

LGAD: Electrical behavior investigation (1)

This work has been supported by the Italian PRIN MIUR 2017 "4DInSiDe" under GA No 2017L2XKTJ, by the European Union's Horizon 2020 Research and Innovation programme under GA No 101004761 "eXFlu-innova" and it has been conducted in collaboration with the INFN CSN5 "eXFlu" research project.

- ❑ **FBK LGADs** (UFSD2, W1)
  - ❑ 55 µm thick
- ❑ **HPK LGADs** (HPK2, split 1-2)
  - ❑ 50 µm thick
- ❑ Simulations-Measurements comparison for not irradiated and irradiated devices.
- ❑ TCAD settings:
  - ❑ "PerugiaModDoping"
  - ❑ Massey avalanche model (FBK) and vanOverstraeten-de Man (HPK).
  - ❑ Temperature sets as per experimenta measurements (RT not irrad, 248 K irrad).

FBK LGADs

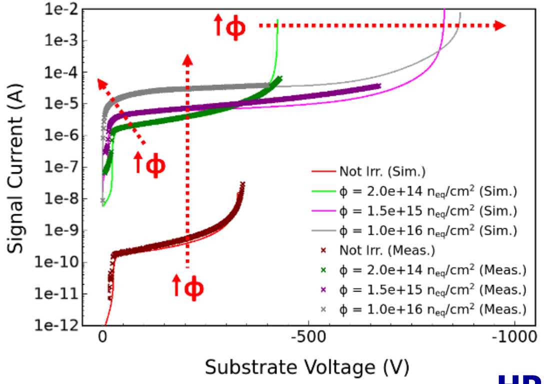

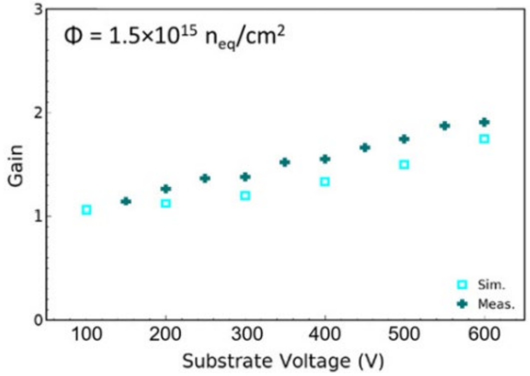

HPK LGADs

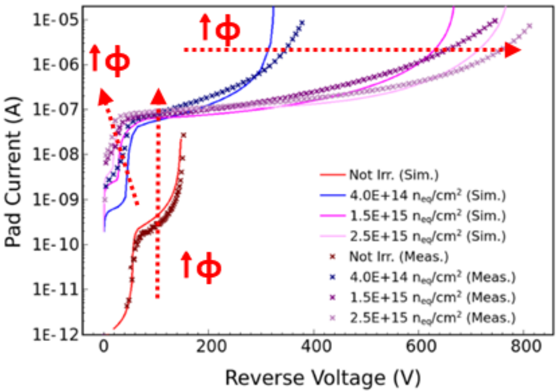

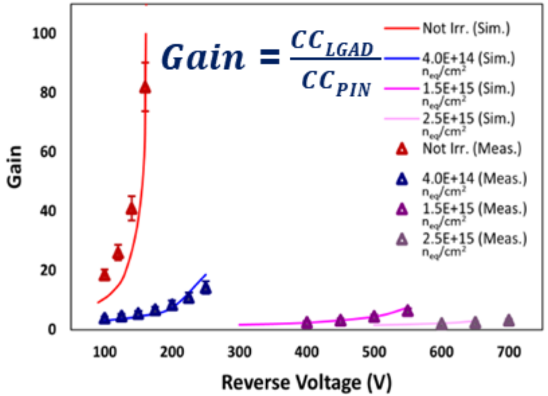

arianna.morozzi@pg.infn.it

Compensated LGAD: innovation for extreme fluences

- Difficult to operate silicon sensors above 10^{16} n_{eq}/cm^2 due to:
  - defects in the silicon lattice structure → dark current increase
  - trapping of the charge carriers → charge collection efficiency decrease
  - change in the bulk effective doping → impossible to fully deplete the sensors
- In standard LGAD
  - acceptor removal mechanism → $\Phi > 1–2 \cdot 10^{15}$ n_{eq}/cm^2 lose the multiplication power and behave as standard n-in-p sensors .
- Overcome the present limits above extreme fluences[6]:
  - saturation of the radiation damage effects above $5 \cdot 10^{15}$ n_{eq}/cm^2
  - the use of thin active substrates (20 – 40 mm)
  - extension of the charge carrier multiplication up to $5 \cdot 10^{17}$ n_{eq}/cm^2

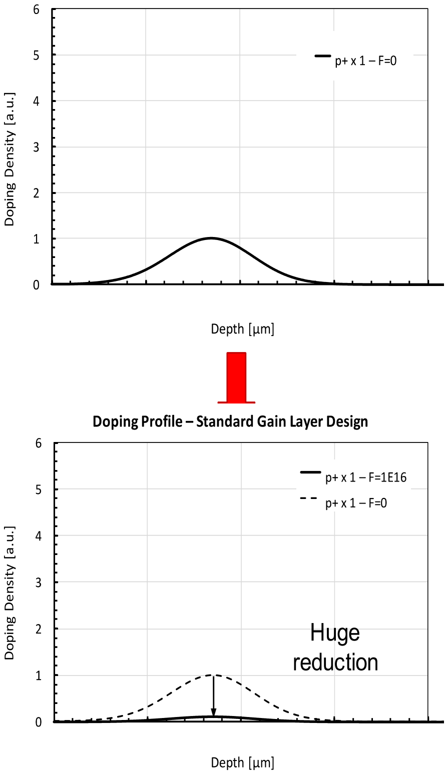

Standard LGAD design

Compensated LGAD: innovation for extreme fluences

- **Goal**: extreme fluences $\Phi = 5 \cdot 10^{17}$ n_{eq}/cm^2
- Impossible to reach the design target with the present design of the gain layer.
- Use the interplay between acceptor and donor removal to keep a constant gain layer active doping density.
  Compensated LGAD: Technology under development (FBK EXFLU1 R&D)
- Many unknowns:
  - donor removal coefficient,
  - interplay between donor and acceptor removal (c_D vs c_A)
  - effects of substrate impurities on the removal coefficients

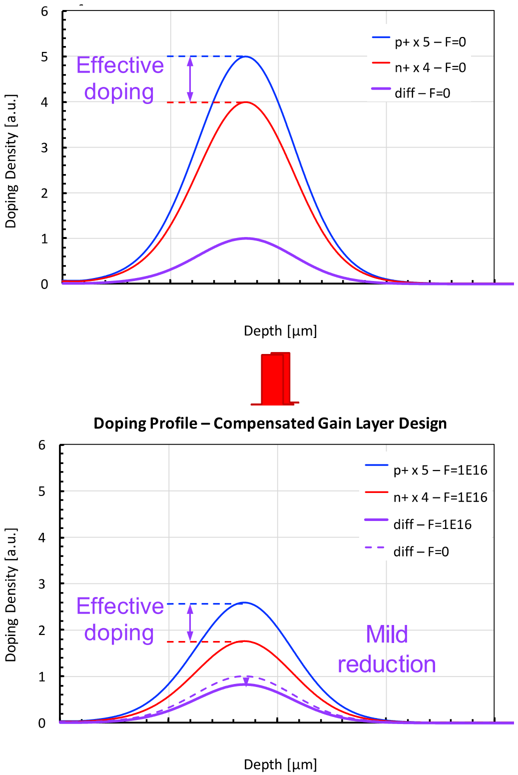

Compensated LGAD

V. Sola et al., NIM A 1040 (2022) 167232.
T. Croci et al., NIM A 1047 (2023) 167815.

arianna.morozzi@pg.infn.it

Compensation – doping evolution with fluence

- ☐ Three scenarios of net doping evolution are possible, according to the acceptor and donor removal interplay:

1. $c_A \sim c_D$

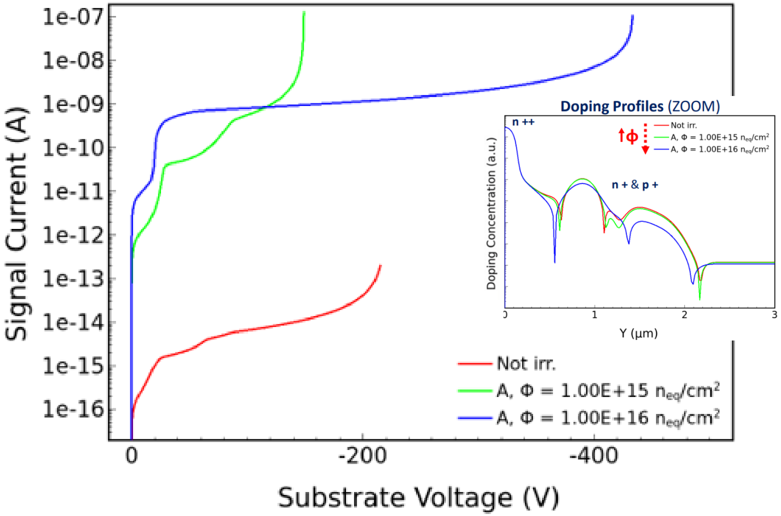

2. $c_A < c_D$
   rapid increase of the net p+-doping → the gain increases with irradiation.
   Co-implantation of oxygen might mitigate the donor deactivation rate.

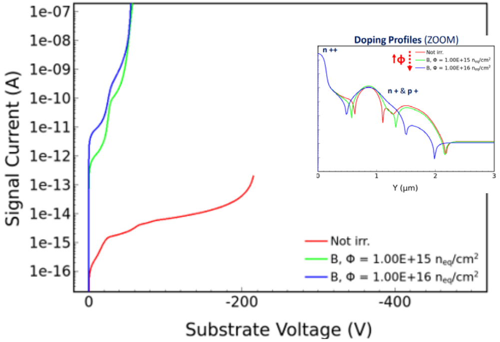

3. $c_A > c_D$
   effective doping disappearance is slower than in the standard design.
   Co-implantation of carbon atoms can mitigate the p+-doping removal.

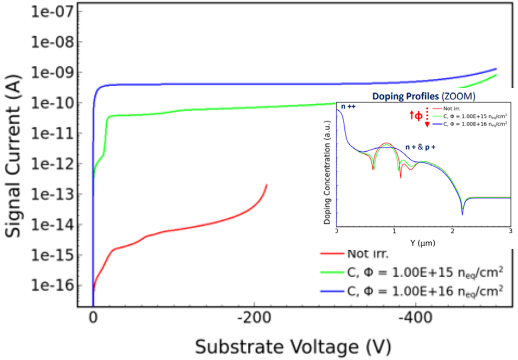

INFN

arianna.morozzi@pg.infn.it

Resistive Silicon Detectors (RSDs)

AC-RSD LGAD

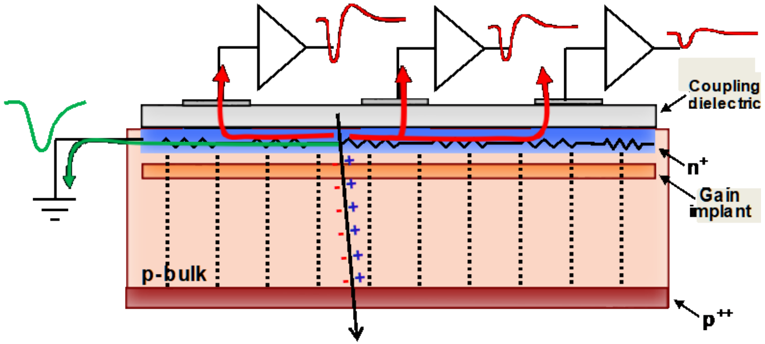

- ✓ This design has been manufactured in several productions by FBK, BNL, and HPK.

1. Long-tail bipolar signals
2. Baseline fluctuation
3. Uncontrolled signal spreading
4. Not easily scalable to large-area sensors

[R. Arcidiacono et al., NIM A 1057 (2023), 168671](#)

DC-RSD LGAD

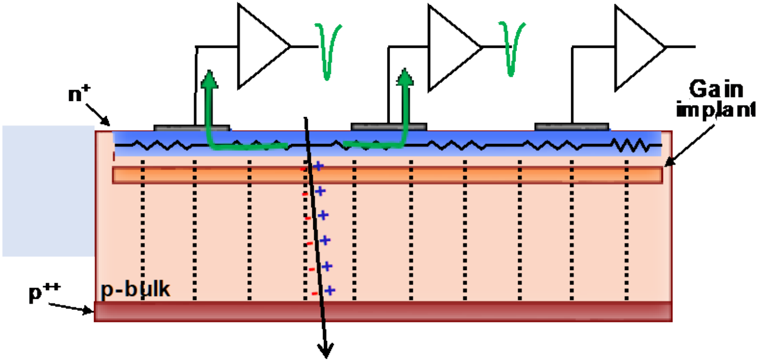

- ✓ Design actually under development by FBK.
- ✓ Promising solution for 4D tracking.

1. Unipolar signals
2. Absence of baseline fluctuation
3. Controlled signal spread
4. Large sensitive areas

- ✓ Evaluation of different layouts and technologies for future DC-RSD production using TCAD tools;

arianna.morozzi@pg.infn.it

Different n^{++} layer resistance

✓ 3D structure, 2x2 PADs => LGAD

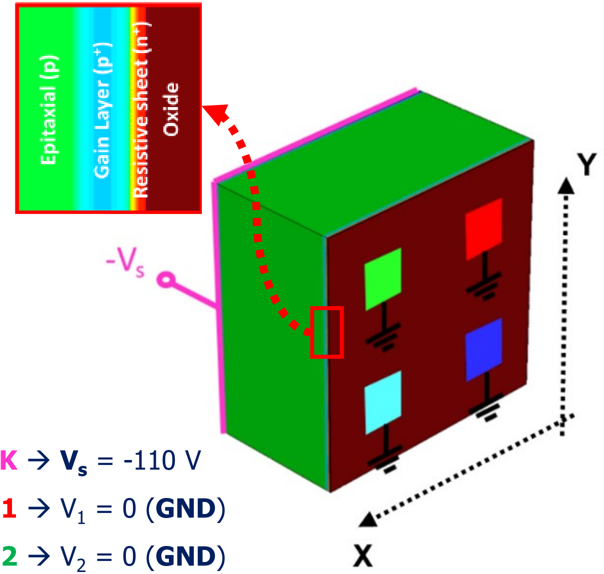

- ☐ **BACK** → $\mathbf{V_s}$ = -110 V
- ☐ **PAD1** → V_1 = 0 (**GND**)
- ☐ **PAD2** → V_2 = 0 (**GND**)
- ☐ **PAD3** → V_3 = 0 (**GND**)
- ☐ **PAD4** → V_4 = 0 (**GND**)

I-V, not irr.

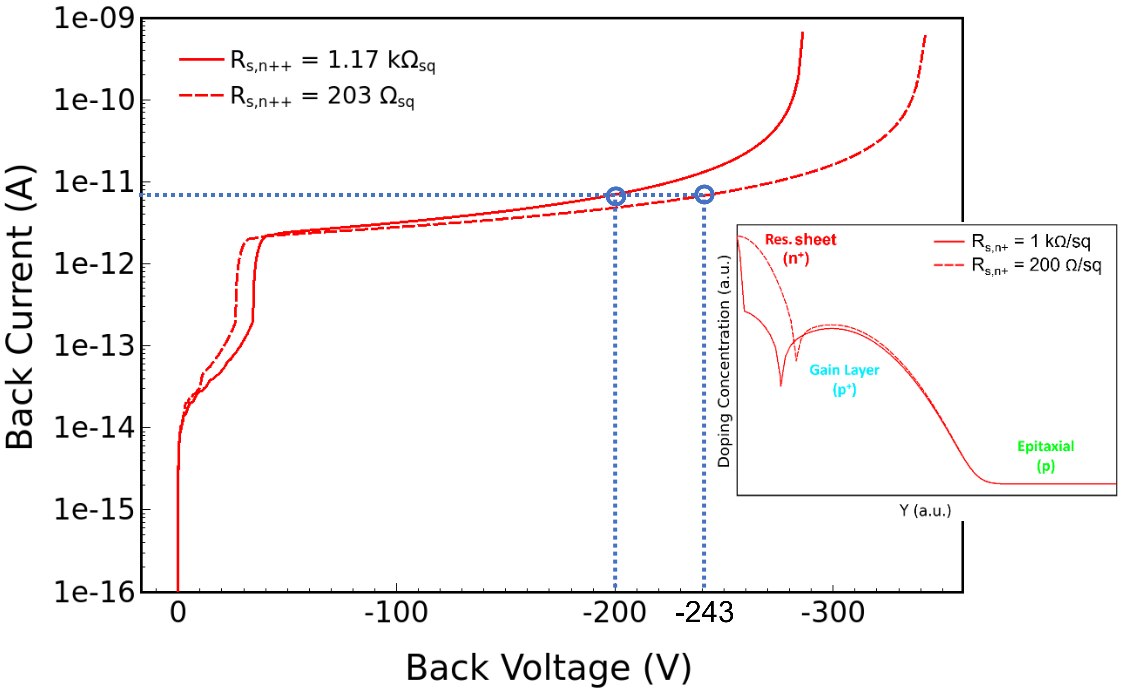

Avalanche model: **Massey**. Temperature **300 K**

arianna.morozzi@pg.infn.it

Heavy Ion model description

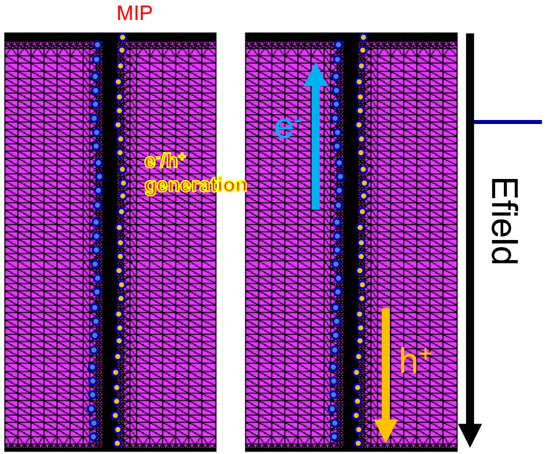

- ❑ Transient time simulation to study the active behavior of detectors.
- ❑ HeavyIon model.

```
HeavyIon(
  Time = 1e-9
   Location =(0,0)
   Direction =(0,1)
   Let_f = @LET_f_pC@
   Length = 60
   Wt_hi = 0.25
   Picocoulomb)
```

- ❑ After the heavy ion impinges the device across a specified particle path, electron-hole pairs are generated and by means of drift-diffusion mechanisms reach the collect contacts.

Transient simulation

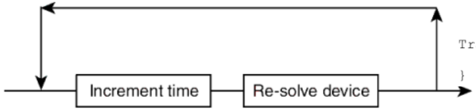

```
Transient( InitialTime = 0.0 FinalTime=1.0e-5 ){
   Coupled { Poisson Electron Hole }
}
```

arianna.morozzi@pg.infn.it

Effect of the PAD shape

- ❑ The DC-RSD design can consider resistors between the read-out electrodes.

→ these resistors could improve the position resolution of the sensors

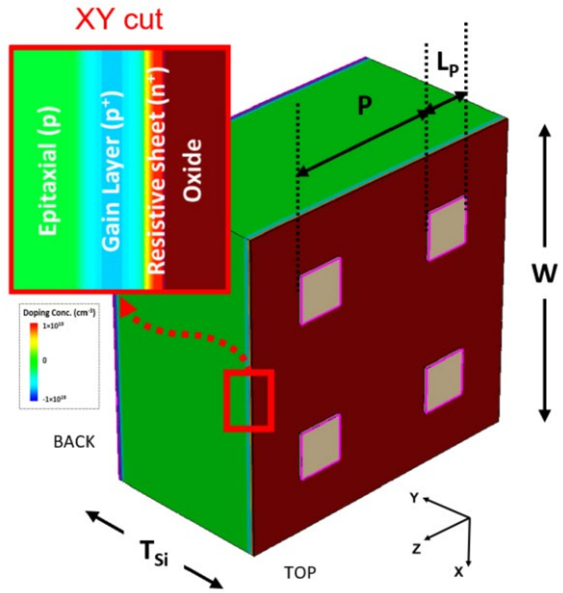

Fig. 8

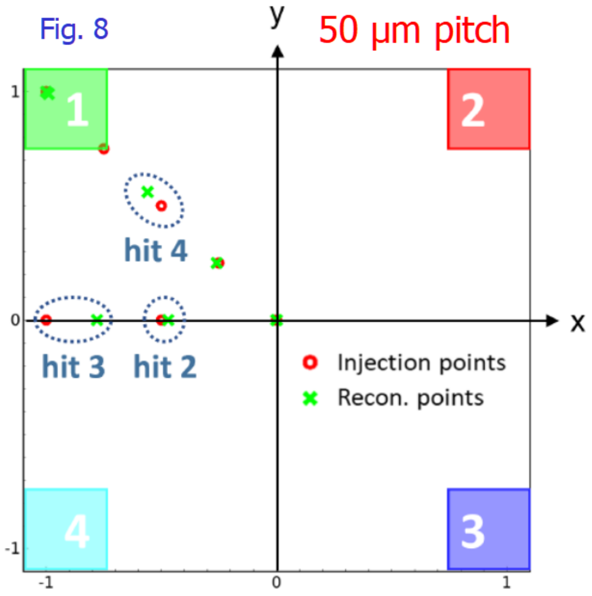

Fig. 9

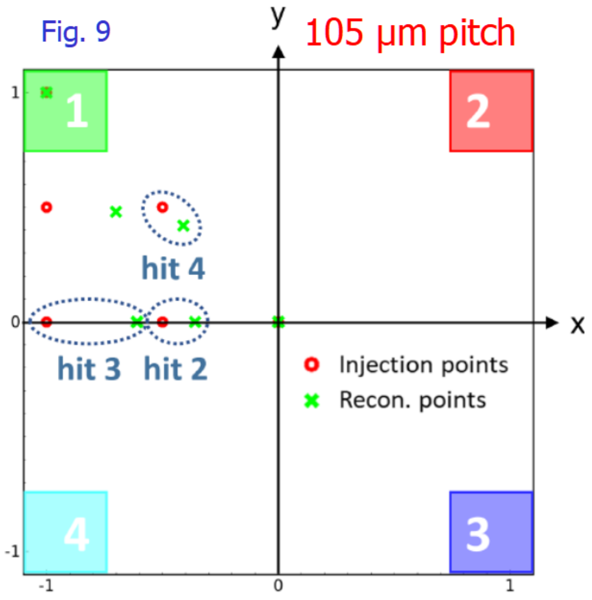

Reconstruction

- ✓ Stimulus MIP
- ✓ The position is reconstructed using the charge imbalance

$$x_i = \frac{Q_{top\,right} + Q_{bottom\,right} - Q_{top\,left} - Q_{bottom\,left}}{Q_{tot}}$$

$$z_i = \frac{Q_{top\,right} + Q_{top\,left} - Q_{bottom\,left} - Q_{bottom\,right}}{Q_{tot}}$$

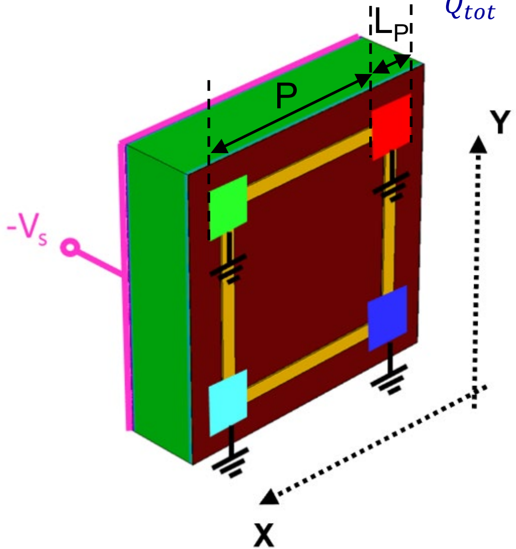

L_P= 15 µm

P = 105 µm

@ V_{Back} = -110 V

$R_{s,n++} \approx$ 721 Ω_{sq}

$R_{s,strip} \approx$ 15 mΩ/µm

Results from *TCAD* simulations

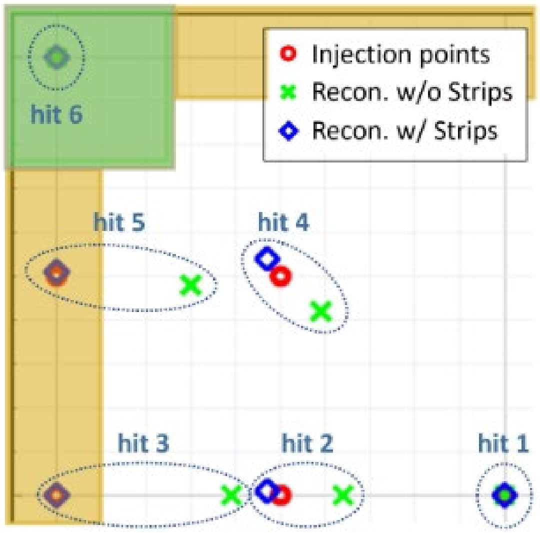

Avalanche model: **Massey**. Temperature **300 K**

Investigate the effect of the contact resistance

- ❑ Investigation of the signal confinement within the TCAD environment.
- ❑ Minimum Ionizing Particle (MIP): various hit points considered.

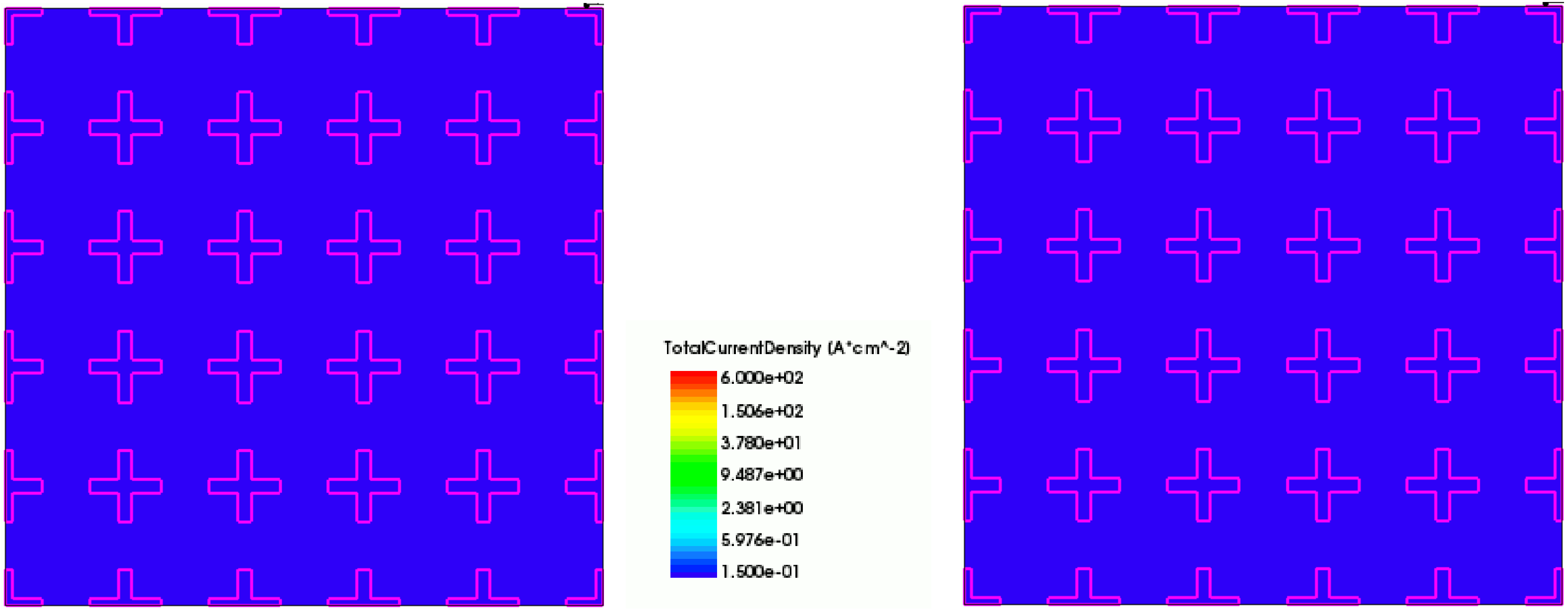

Contact resistance $= 10\ \Omega$

Contact resistance $= 1\ k\Omega$

arianna.morozzi@pg.infn.it

Investigate the effect of the contact shape

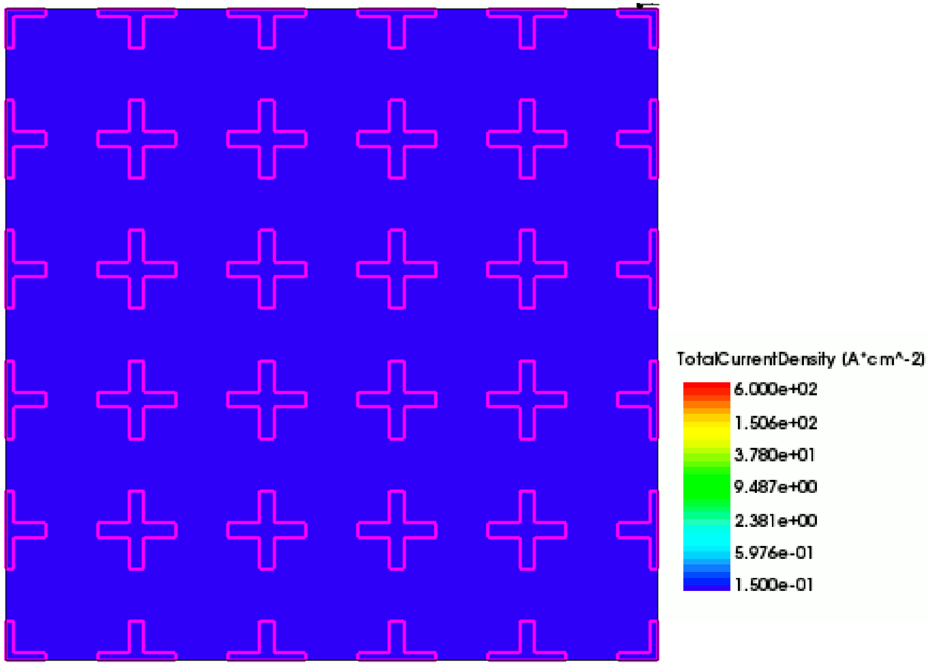

36 electrodes

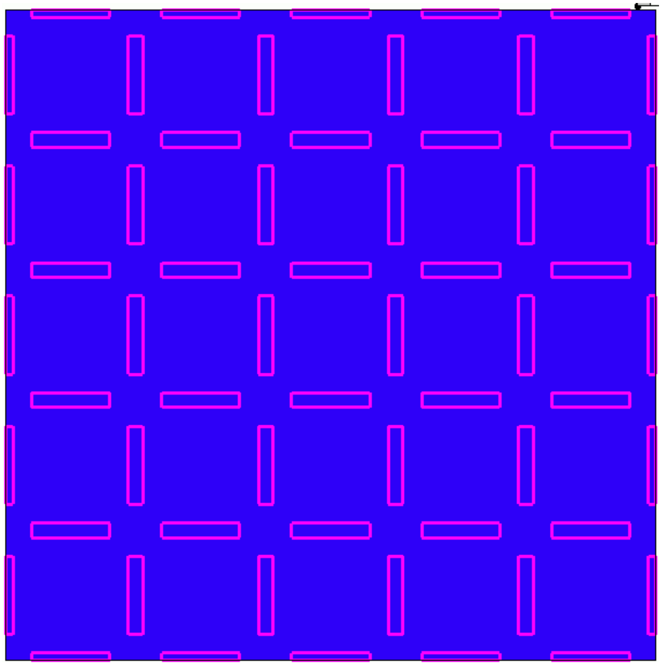

60 electrodes

Inter-pad resistors

A single resistance strip has a resistance equal to

2% of the sheet resistance

40% of the sheet resistance

375% of the sheet resistance

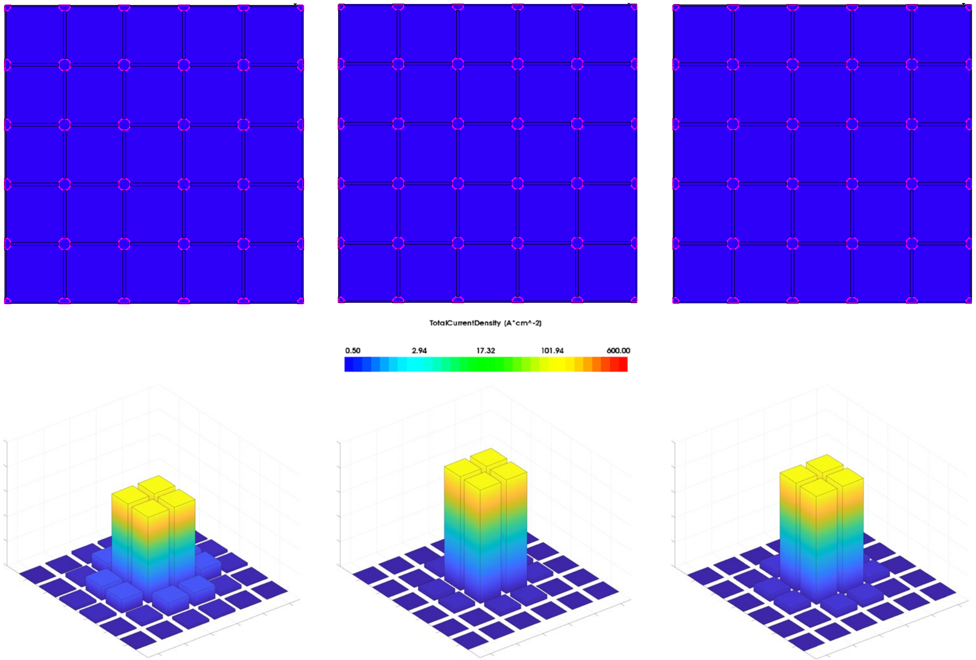

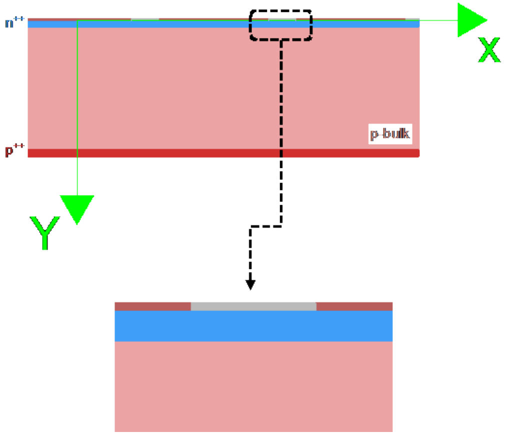

arianna.morozzi@pg.infn.it

Isolating trenches

- The small losses in the current density map are probably due to the small pixels.
- The charge is in turn collected almost entirely by the four pads of the affected pixel.
- Trench interrupting the resistive n++ layer excellently confines the signal.

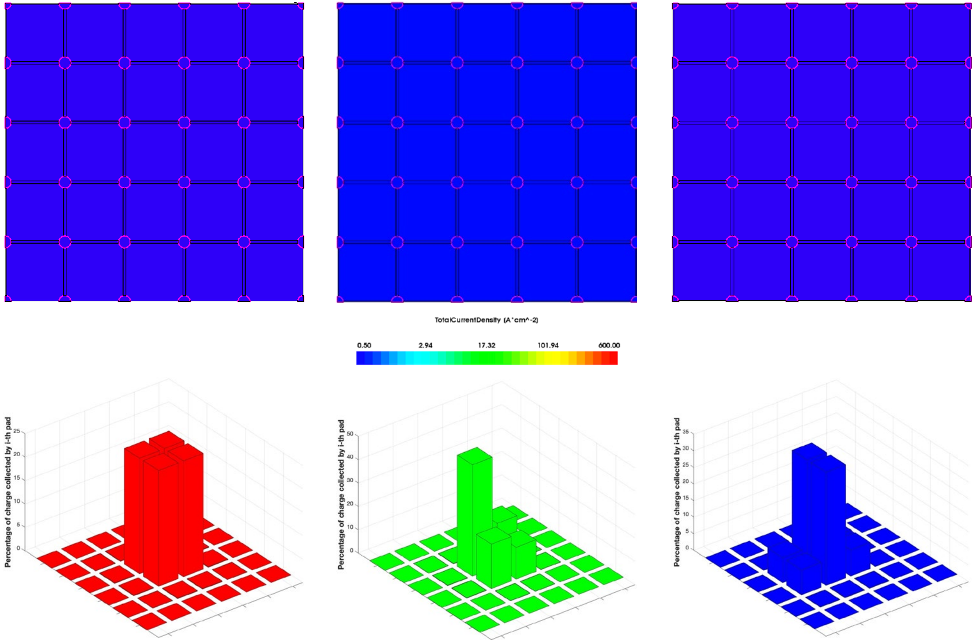

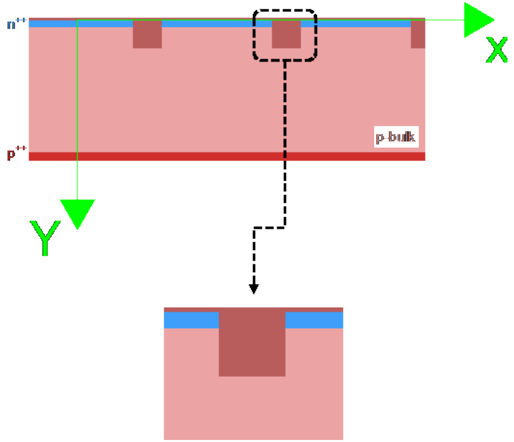

arianna.morozzi@pg.infn.it

Charge sharing and signal confinement

- ❑ Different pad geometries
  - Cross or bar-shaped;
  - Better confinements in larger pads;
  - Small electrodes to avoid introducing distortions in the reconstruction of the impact position
  - Error in reconstruction by associating any point covered by metal with the center of the pad;
  - Need small, circular-shaped electrodes and a strategy to confine the signal (e.g., trenches);

Three hit points

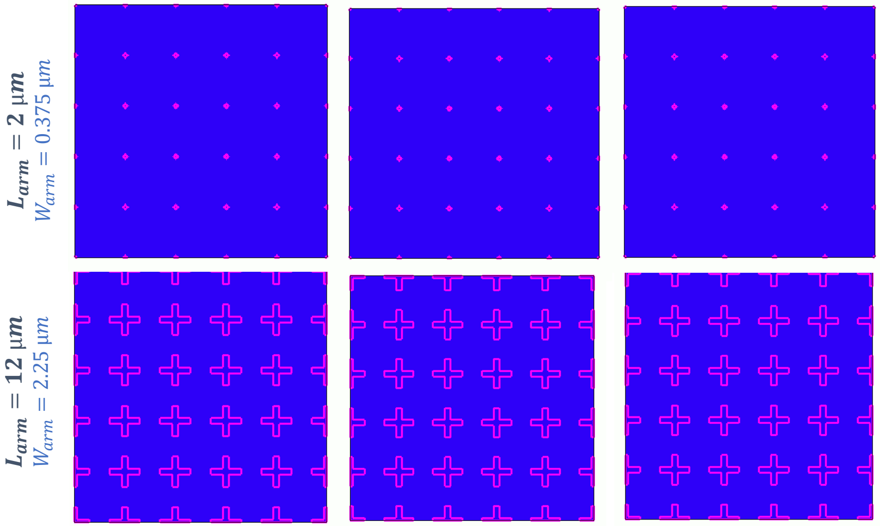

arianna.morozzi@pg.infn.it

ARCADIA sensors in 110 nm CMOS technology

- Large-area **monolithic pixel detectors for particle tracking**: low power, high rate capability, low cost per unit area, low material budget
- Target **applications**:
  - Medical imaging (e.g. Proton Computed Tomography)
  - Astro-particle detection on satellites
  - High Energy Physics experiments
- Customized **110nm CMOS** process (LFoundry)
- n-type **high resistivity** active region
- Reverse-biased **junction at the bottom**: depletion grows from back to top
- **Sensing** electrodes can be biased at **low voltage** (< 1V)
- nwells with electronics shielded by **deep pwells**
- **n-epi** layer: reduce **punch-through** current between p+ and deep pwells

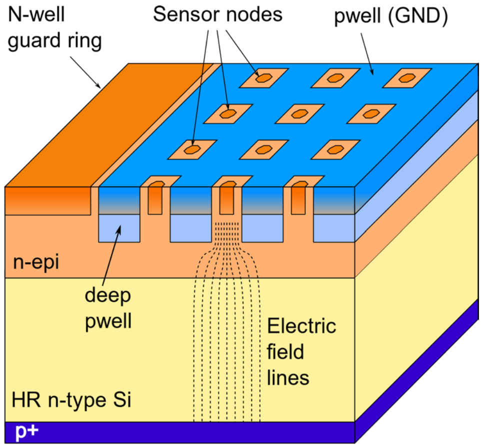

Material courtesy of L. Pancheri

arianna.morozzi@pg.infn.it

ARCADIA sensors in 110 nm CMOS technology

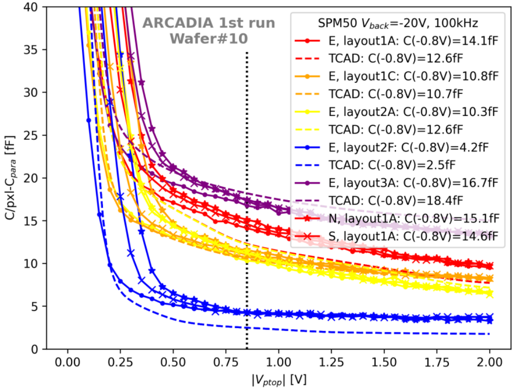

Experimental data for different pixel layouts comparison with **TCAD simulation results**

Capacitance is dominated by the **perimeter** of the sensor node

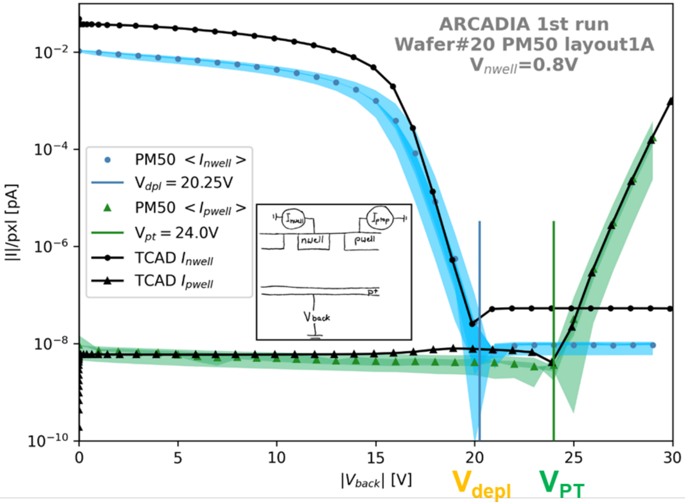

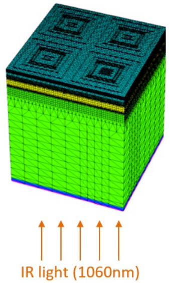

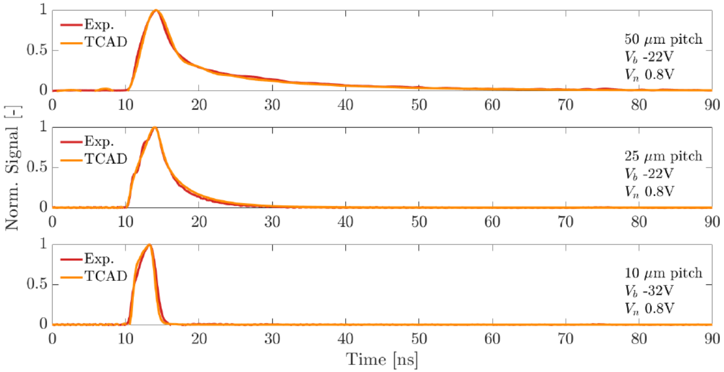

IR laser diode @ 1060nm, < 100ps FWHM: generation in the whole active thickness

Pixel array test structures with **100μm active thickness** (maskless backside p+ implantation)

L. Pancheri et al., IEEE Transactions on Electron Devices, 67(6) (2020).
T. Corradino et al., Frontiers in Physics, vol. 10, 2022,
C. Neub¨user et al., JINST 18(01) C01066 (2023)

arianna.morozzi@pg.infn.it

Monolithic detectors (MAPS): OVERMOS project

OVERMOS is a **CMOS MAPS (Monolithic Active Pixel Sensor)** project demonstrator fabricated using:

- TJ 180 nm Hi-res 18 um thick epitaxial layer 1kOhm –cm
- Small (3.5x3.5 um2) n-collecting nodes
- Multi diode arrangements within pixel
- CMOS DPW ~ originally proposed for DECAL of ILC
- OVERMOS devices have been n-irradiated to Φ [1e13,5e13,1e14,5e14,1e15]

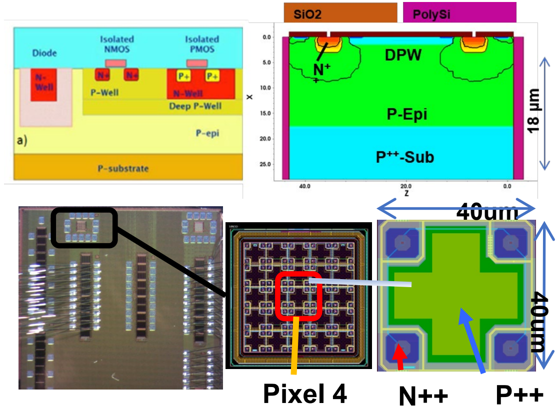

Physics models: SDEVICE parameters for mobility and recombination

- Temp = 21°C
- Fermi
- SRH (DopingDep,TempDep, ElectricField (Lifetime = Hurkx)
- Mobility(PhuMob Enormal (Lombardi PosInterfaceCharge)
- HighFieldSaturation(EParallel)
- RefDens_eEparallel_ElectricField_HFS= 1e17
- UniBo for impact ionization (incl. Auger, Eparallel)
- Same RefDens for interpolation of Fava to F
- Excluded flat elements by increasing TOX (or using FlatElementExclusion)

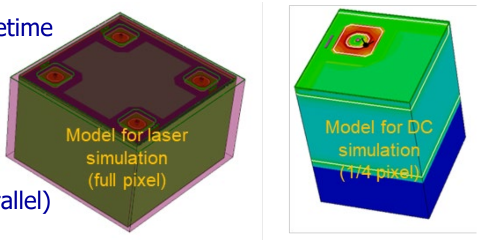

Math models

- ILS
- ParallelToInterfaceInBoundaryLayer(FullLayer -ExternalBoundary)
- Geometricdistances **at interfaces*
- e/hMobilityAveraging=ElementEdge * *for interface mobility degradation*)
- TrapsDLN=30
- Traps(Damping=100)

Radiation models

- HPTM

Interface effects considered

- Fixed oxide-charge (**Oxch**) density and interface traps (**Oxint**) included
- Interface traps distributed among 3 energy levels, Gaussian , σ = 70meV
- Ratio Oxint/Oxch ~ 0.9
- Simulations 1.2e11 Oxch
- Xsection 1E-15 cm^-2

Material courtesy of F.R. Palomo, VERTEX2019

"TCAD Processes and device simulations of OVERMOS, a CMOS 180nm MAPS detector", E.G.Villani, 34th RD50 Workshop, Lancaster University, UK, 12-14 June 2019

arianna.morozzi@pg.infn.it

OVERMOS MAPS TCAD Simulation results

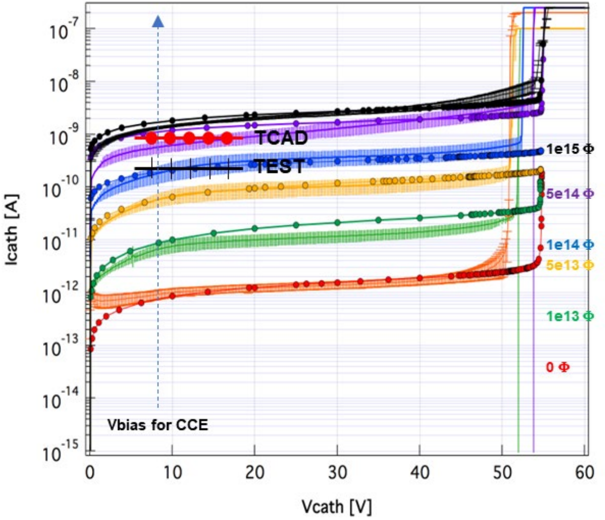

DC IV plots up to BV

<IV>[10] measured OVERMOS + σ

IV TCAD Oxch 1.2e11, OxINT 1.1e11

Φ	I_{leak_μ}[A] @10V	I_{leak_TCAD}[A] @10V	Δ%	${}^{a}BV_{\mu}$[V]	BV_{TCAD}[V]
0	1.0e-12	0.85e-12	15	50.8	54.79
1e13	7.5e-12	1e-11	-33.3	52	54.6
5e13	6.72e-11	7.47e-11	-11.1	51.2	54.7
1e14	2.1e-10	2.06e-10	1.9	52.4	54.7
5e14	6.21e-10	1.18e-9	-90	53.6	54.8
1e15	1.43e-9	1.83e-9	-28	54.4	54.8

^{a}BV defined as V: $(\Delta I/\Delta V)_{max}$

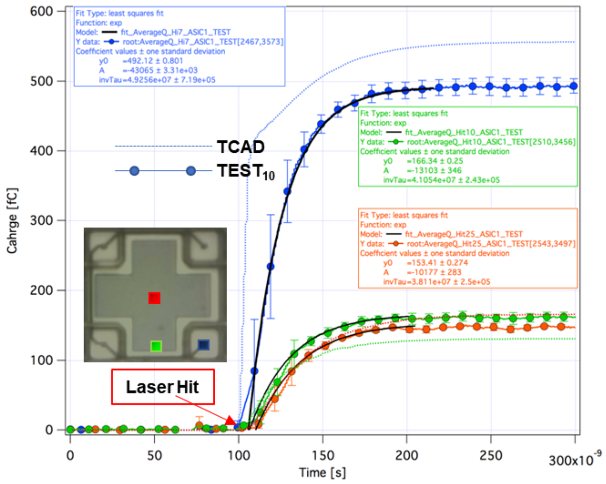

```
Fit Type: least squares fit
Function: exp
Model: fit_AverageQ_Hi7_ASIC1_TEST
Y data: root:AverageQ_Hi7_ASIC1_TEST[2467,3573]
Coefficient values ± one standard deviation
    y0     =492.12 ± 0.801
    A      =-43065 ± 3.31e+03
    invTau=4.9256e+07 ± 7.19e+05

Fit Type: least squares fit
Function: exp
Model: fit_AverageQ_Hit10_ASIC1_TEST
Y data: root:AverageQ_Hit10_ASIC1_TEST[2510,3456]
Coefficient values ± one standard deviation
    y0     =166.34 ± 0.25
    A      =-13103 ± 346
    invTau=4.1054e+07 ± 2.43e+05

Fit Type: least squares fit
Function: exp
Model: fit_AverageQ_Hit25_ASIC1_TEST
Y data: root:AverageQ_Hit25_ASIC1_TEST[2543,3497]
Coefficient values ± one standard deviation
    y0     =153.41 ± 0.274
    A      =-10177 ± 283
    invTau=3.811e+07 ± 2.5e+05
```

Q_{coll}	Test	TCAD	Δ%
<Qh7>	492	556	**-13**
<Qh10>	166	131	**21**
<Qh25>	153	166	**-8.4**

SDEVICE Optical Generation parameters:

- OpticalGeneration (QuantumYield (StepFunction (EffectiveBandgap))
- ComplexRefractiveIndex (CarrierDep(Imag) WavelengthDep(Imag)) * extinction coeff. only
- OpticalSolver (OptBeam (LayerStackExtraction (WindowName = "LaserW" Position = (0, Y_hit, Z_hit) Mode = ElementWise * Laser window of 5 x 5 um2, centre position retrieved from .gds, default NumberOfCellsPerLayer
- Wavelength= 1.064 * Incident light wavelength [um]
- Intensity= @<20000.0*exp(-0.036*@Silicide_Thick@)*0.966>@ PolarizationAngle= 0 Theta= 90 Phi = 0

- The models seems to predict leakage current for the Tower Jazz 180nm SL CMOS process.
- Breakdown Voltage (BV) needs improvement.

Material courtesy of F.R. Palomo, VERTEX2019

arianna.morozzi@pg.infn.it

Radiation damage models

Synopsys Sentaurus TCAD Sdevice simulations
for HEP experiments

arianna.morozzi@pg.infn.it

TCAD models - an overview

Different approaches to TCAD radiation damage modeling:

✓	EVL Model	(2 levels)
✓	Delhi-2014	(2 levels)
✓	KIT (Eber)	(2 levels)
✓	New Univ. Of Perugia Bulk+Surface	(3 levels)
✓	Folkestad (CERN model)/LHCb	(3 levels)
✓	Hamburg Penta Trap Model (HPTM)	(5 levels)

Different modeling approaches (traps, energy levels and related parameters), often tailored to specific datasets and devices.

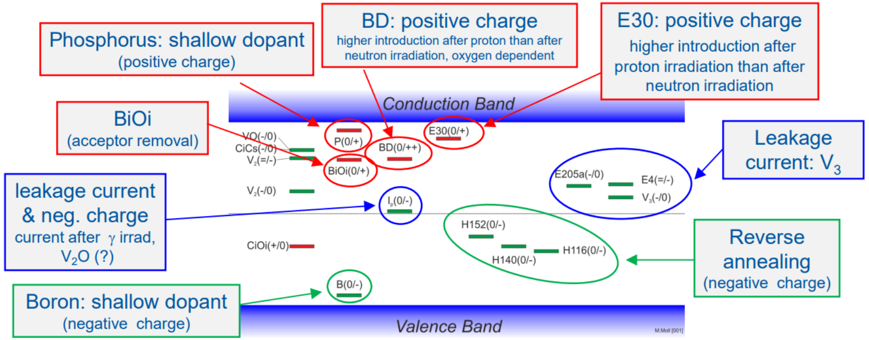

Phosphorus: shallow dopant
(positive charge)

BD: positive charge
higher introduction after proton than after neutron irradiation, oxygen dependent

E30: positive charge
higher introduction after proton irradiation than after neutron irradiation

BiOi
(acceptor removal)

Leakage current: V_3

leakage current & neg. charge
current after γ irrad, V_2O (?)

Reverse annealing
(negative charge)

Boron: shallow dopant
(negative charge)

RD50 map of most relevant defects for device performance near RT

GOAL: General purpose TCAD model (DRD3 WP4 - ECFA Detector R&D Roadmap)

- Not over specific
  → set of "effective" defects within the semiconductor bandgap.
- Predictive capabilities to be extended $\Phi > 10^{16}\ n_{eq}/cm^2$.
- Accounts for different irradiation levels and particle types.

Hamburg Penta Trap Model (HPTM)

- ❑ HPTM with 5 effective traps
  - ❑ Developed to simulate the I-V, C-V and CCE with IR of diodes for various fluence levels and use the TCAD optimizer to determine the free parameters i.e., minimize simultaneously for every fluence.
- ❑ Optimize the performance of pad diodes irradiated with 24 GeV/c p in the fluence range of $3{\cdot}10^{14}$ to $1.3{\cdot}10^{16}$ n_{eq}/cm^{-2}.
- ❑ Charge trapping is essential to predict the response of radiation-damaged segmented sensors, due to the highly non-uniform weighting field.

Result of tuning: Hamburg Penta Trap Model (HPTM)

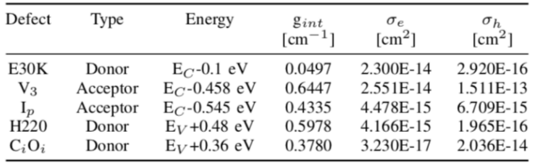

Defect	Type	Energy	g_{int} [cm^{-1}]	σ_e [cm^2]	σ_h [cm^2]
E30K	Donor	E_C-0.1 eV	0.0497	2.300E-14	2.920E-16
V_3	Acceptor	E_C-0.458 eV	0.6447	2.551E-14	1.511E-13
I_p	Acceptor	E_C-0.545 eV	0.4335	4.478E-15	6.709E-15
H220	Donor	E_V+0.48 eV	0.5978	4.166E-15	1.965E-16
C_iO_i	Donor	E_V+0.36 eV	0.3780	3.230E-17	2.036E-14

- Trap concentration of defects: $\mathbf{N = g_{int} \cdot \Phi_{neq}}$
- Simulations for the optimization have been performed at **T= -20 °C** with:
  1. Slotboom band gap narrowing
  2. Impact ionisation (van Overstaeten-de Man)
  3. Trap Assisted Tunneling Hurkx with tunnel mass = **0.25 m_e** (default value: 0.5 m_e) in case of the I_p
  4. Relative permittivity of silicon = 11.9 (default value: 11.7)
- Both cross section for the E30K and the electron cross section for the C_iO_i were fixed ➔ 12 free parameter
- Optimization done with the nonlinear simplex method

Comparison with strips

Simulated structure

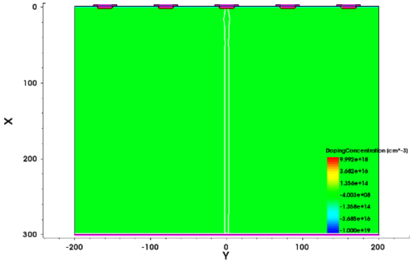

Collected charge vs. fluence

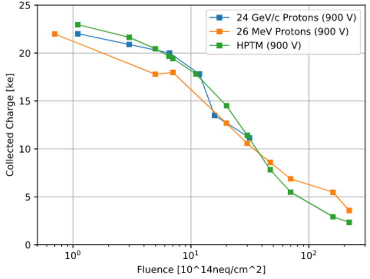

- Float zone silicon
- 300 um thick sensors
- 80 um pitch
- T = -25 °C
- ^{90}Sr source

Data from A. Affolder et al., NIMA Vol. 623 (2010), pp. 177-179.

J. Schwandt, arXiv:1904.10234.
J. Schwandt, IEEE NSS MIC 2028 talk.

arianna.morozzi@pg.infn.it

HPTM Simulation results

I-V for fluences from 0.3 - 13•10^{15} n_{eq}/cm² at T= -20 °C (for T= -30 °C see backup)

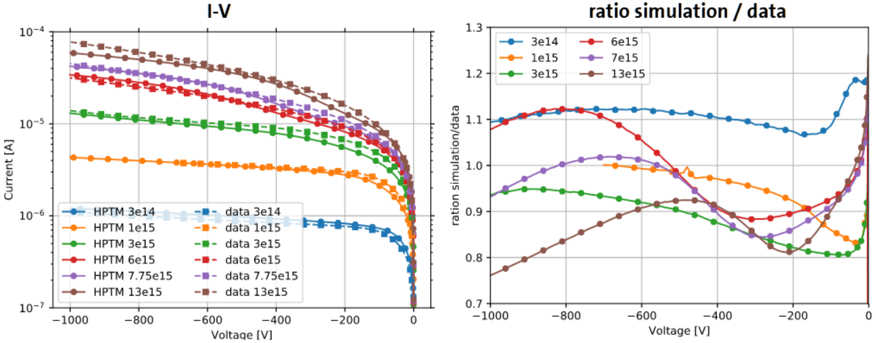

C-V for fluences from 0.3 - 13•10^{15} n_{eq}/cm² at 455 Hz and T = -20 °C (for T= -30 °C see backup)

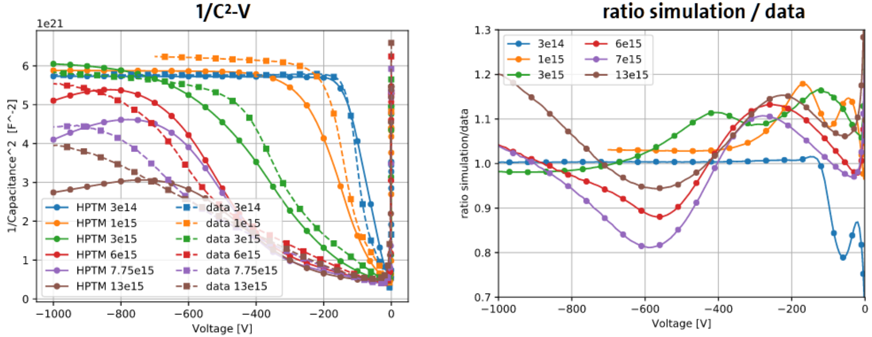

CCE vs. V for fluences from 0.3 - 13•10^{15} n_{eq}/cm² with infrared laser and T = -20 °C (for T= -30 °C see backup)

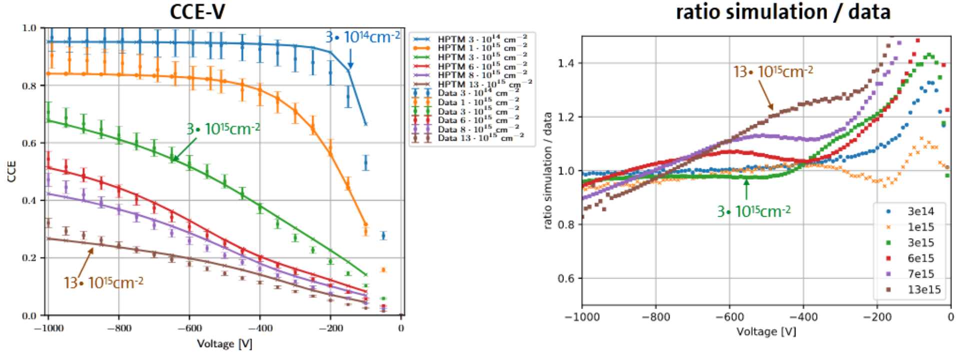

T= -20°C, 60min at 80°C

[J. Schwandt, arXiv:1904.10234.](https://arxiv.org/abs/1904.10234)
J. Schwandt, IEEE NSS MIC 2028 talk.

CERN bulk radiation damage model (Falkestad)

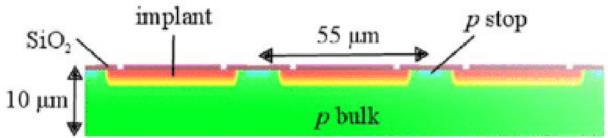

From the classical **EVL model***, one donor and one acceptor level (1 and 2 in the table), they add a third acceptor level. Cross-sections are adjusted to experimental results. Measurements for 200 μm thick n-on-p sensors bump bonded to TimePix3 readout .

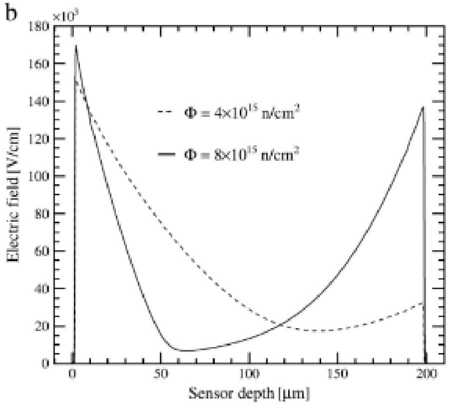

Simulated electric field (2D mesh) in pixel centre at 1000V bias for two fluence levels.

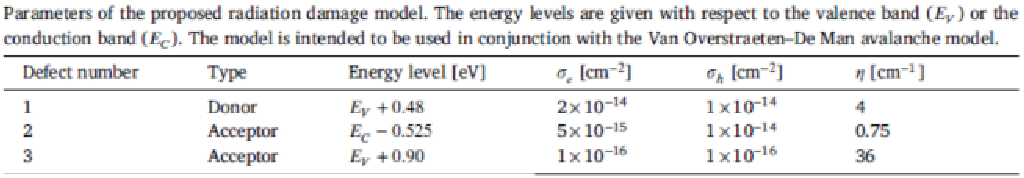

Parameters of the proposed radiation damage model. The energy levels are given with respect to the valence band (E_V) or the conduction band (E_C). The model is intended to be used in conjunction with the Van Overstraeten–De Man avalanche model.

Defect number	Type	Energy level [eV]	σ_e [cm^{-2}]	σ_h [cm^{-2}]	η [cm^{-1}]
1	Donor	$E_V + 0.48$	2×10^{-14}	1×10^{-14}	4
2	Acceptor	$E_C - 0.525$	5×10^{-15}	1×10^{-14}	0.75
3	Acceptor	$E_V + 0.90$	1×10^{-16}	1×10^{-16}	36

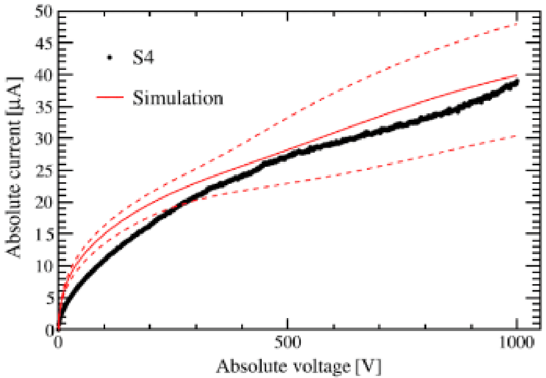

Measured and simulated I-V curves (T=-31,1ºC) after uniform proton irradiation to Φ=4e15 MeV n$_{eq}$/cm^2.

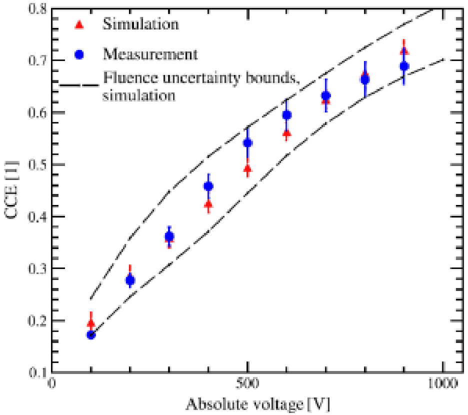

Measured and simulated CCE as a function of voltage at Φ=4e15 MeV n$_{eq}$/cm^2.

The model captures the transition from a linear electric field/saturating I-V curve to a double junction electric field/non-saturating I-V curve, as a consequence of avalanche generation in the high-field regions of doublé junctions. For pixel center hit, the CCE is aceptable.

A. Folkestad et al., NIM A 874 (2017) pp. 94-102
F.R. Palomo, VERTEX2019

3Ds

Columnar vs Trench

From planar to 3D

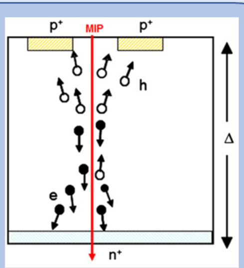

Schematic cross-sections planar sensors

ADVANTAGES:

- Easy to fabricate;
- Low capacitance.

DISADVANTAGES:

- High full depletion voltage;
- Low temporal resolution.

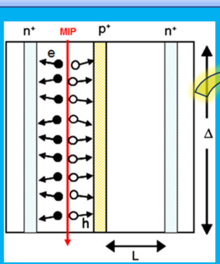

Schematic cross-sections 3D sensors

ADVANTAGES:

- Low depletion voltage;
- High Radiation tolerance.

DISADVANTAGES:

- High capacitance;
- Complicated fabrication technology.

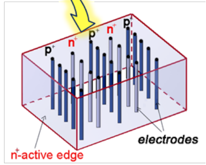

First generation design

Features:
High radiation tolerance;
High fabrication yield.

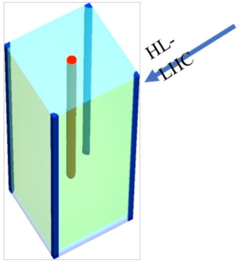

Small pitch 3D pixel sensors

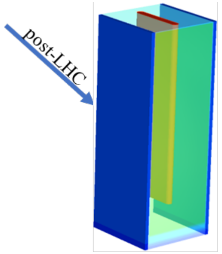

3D trench-electrode sensors

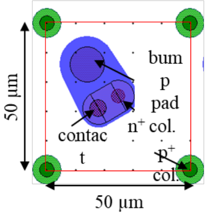

Layout of Small pitch 3D pixel sensors

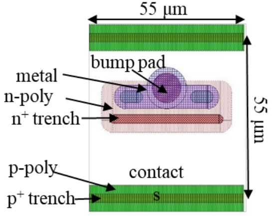

Layout of 3D trench-electrode sensors

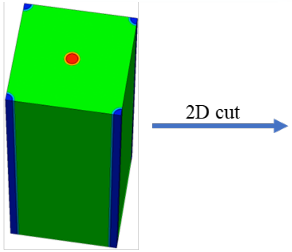

50×50-1E Simulation Domain

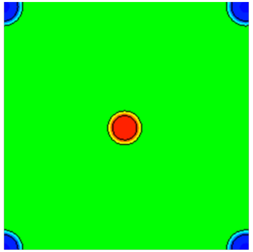

2D cut

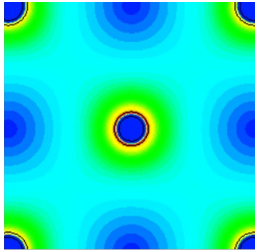

Electric Field, V_b=100V

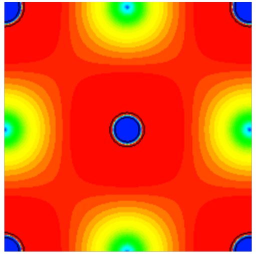

Electron Drift Velocity V_b=100V

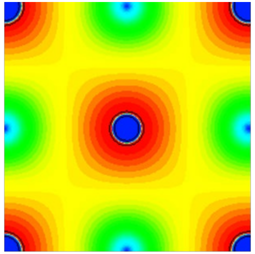

Hole Drift Velocity V_b=100V

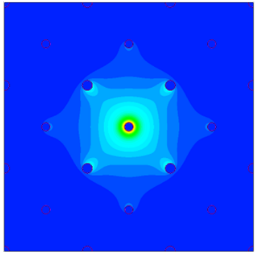

Weighting Field of 3×3 array

Small pitch 3D pixel sensors - - 2D Domain

Material courtesy of G.-F. Dalla Betta

arianna.morozzi@pg.infn.it

Small pitch 3D pixel sensors – 3D Domain

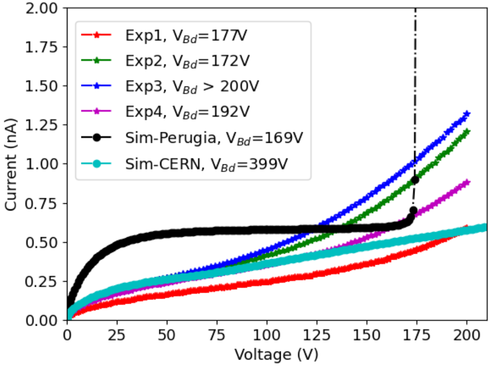

Fluence = 1E16 n_{eq}/cm^2

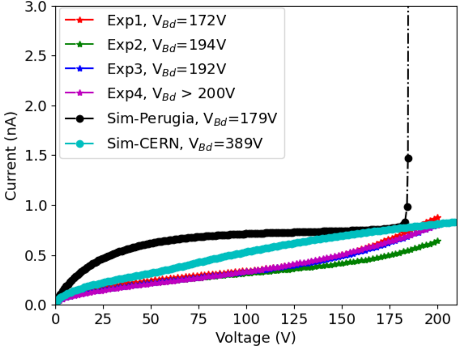

Fluence = 2E16 n_{eq}/cm^2

CERN bulk damage model reproduces better leakage current

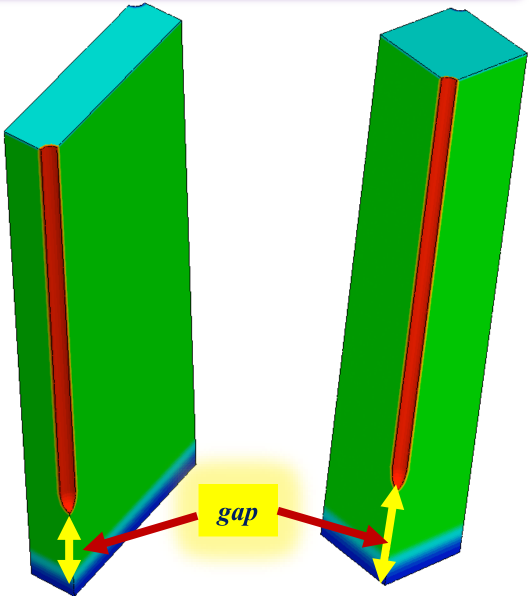

Simulation domain 25×100-1E

Simulation domain 50×50-1E

Perugia bulk damage model is better at predicting the breakdown voltage

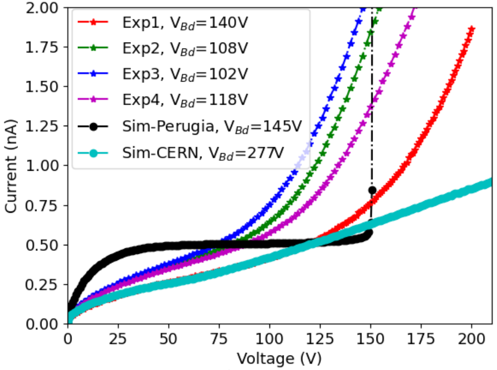

Fluence = 1E16

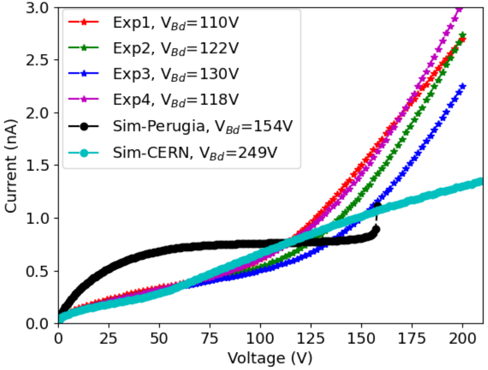

Fluence = 2E16

Material courtesy of G.-F. Dalla Betta

Small pitch 3D pixel sensors – 3D Domain

All the simulations were based on the Perugia Bulk Damage Model

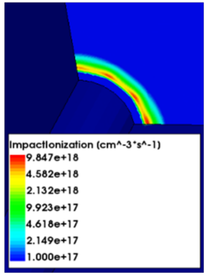

Breakdown on the surface before irradiation

25×100-1E

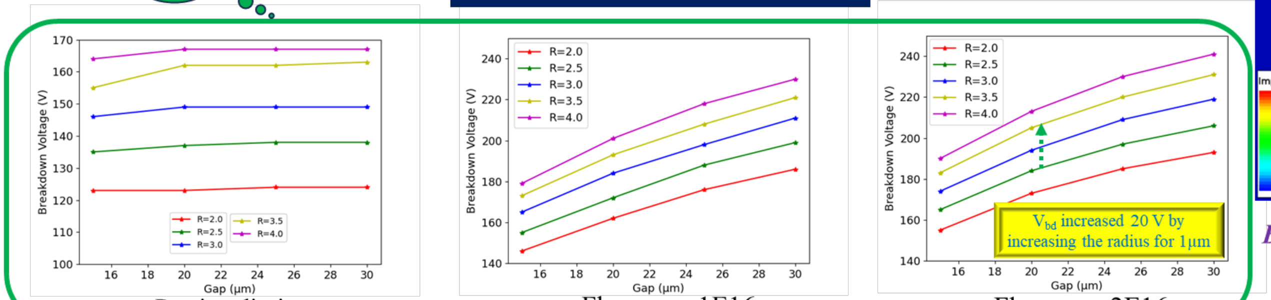

V_{bd} increased 20 V by increasing the radius for 1μm

Pre-irradiation Fluence = 1E16 Fluence = 2E16

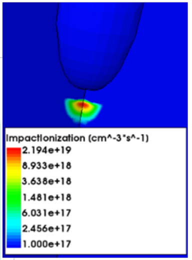

Breakdown on the tip after irradiation

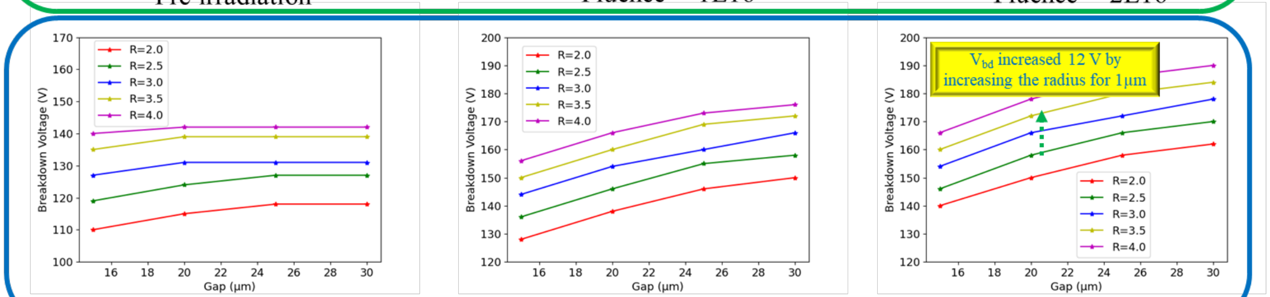

V_{bd} increased 12 V by increasing the radius for 1μm

Pre-irradiation Fluence = 1E16 Fluence = 2E16

50×50-1E

Preliminary conclusion: increase the radius of the electrodes to improve the breakdown voltage

J. Ye et al., Sensors 2023, 23(10), 4732

Material courtesy of G.-F. Dalla Betta

The “New Univ. of Perugia” model - at a glance

√ Surface damage (+ Q_{OX})

Type	Energy (eV)	Band width (eV)	Conc. (cm^{-2})
Acceptor	$E_C \le E_T \le E_C - 0.56$	0.56	$D_{IT} = D_{IT}(\Phi)$
Donor	$E_V \le E_T \le E_V + 0.6$	0.60	$D_{IT} = D_{IT}(\Phi)$

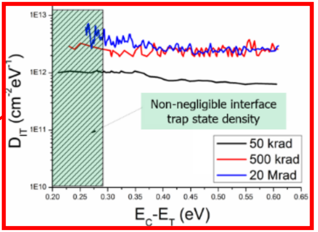

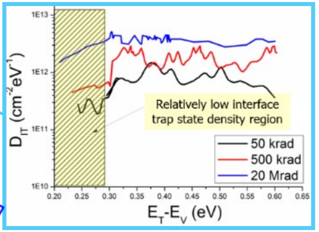

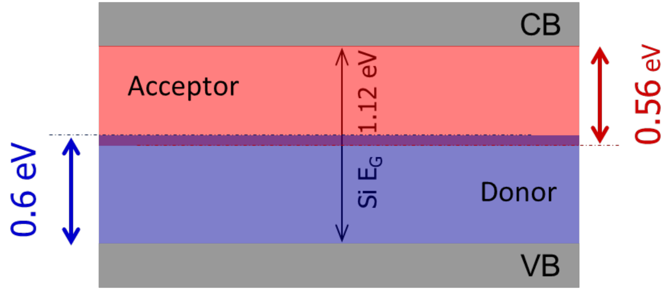

√ Bulk damage

Avalanche ON: Van Overstraeten–De Man (default)

Type	Energy (eV)	η (cm^{-1})	σ_n (cm^2)	σ_h (cm^2)
Donor	E_C - 0.23	0.006	2.3×10^{-14}	2.3×10^{-15}
Acceptor	E_C - 0.42	1.6	1×10^{-15}	1×10^{-14}
Acceptor	E_C - 0.46	0.9	7×10^{-14}	7×10^{-13}

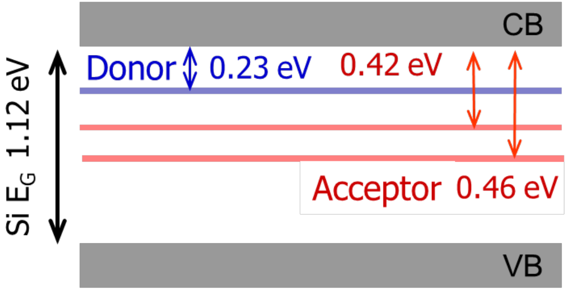

A. Morozzi et al., Front. Phys., 9 (2021)

arianna.morozzi@pg.infn.it

The “New Univ. of Perugia” model – flow

The overall modelling approach pursued

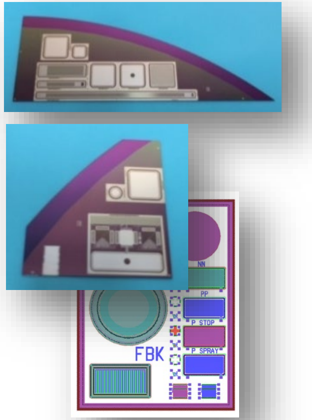

TEST STRUCTURE MEASUREMENTS

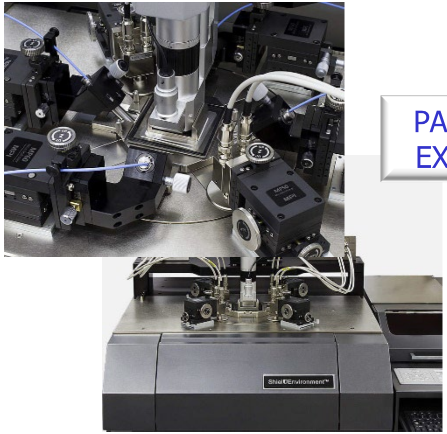

PARAMETERS EXTRACTION

MODEL

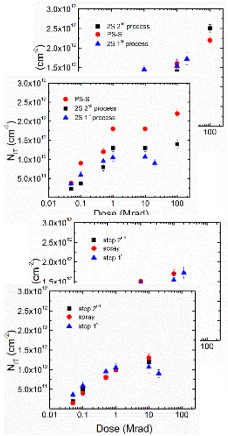

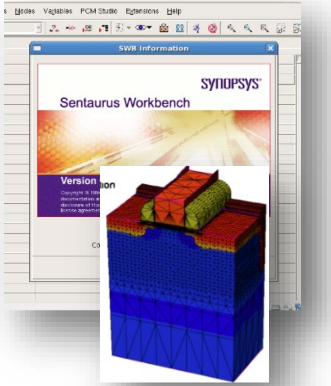

MODEL VALIDATION

DETECTOR OPTIMIZATION

CCE, I-V, C-V, …

- √ Modeling the effects of the radiation damage.
- √ Predictive insight into the behavior of detectors, aiming at their performance optimization.

Surface model validation: MOS capacitors

Measurements
Simulations

IFX MOS Capacitors

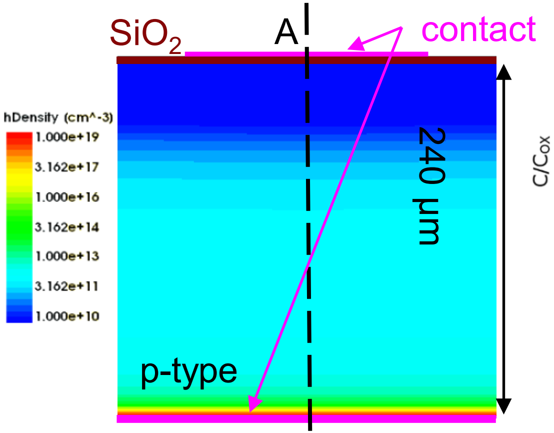

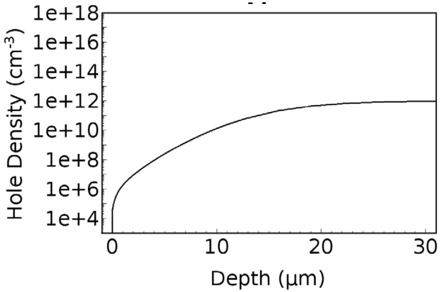

6" process.

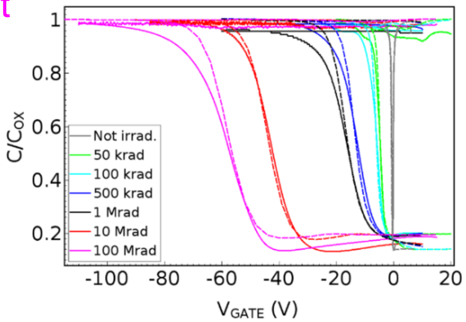

8" process.

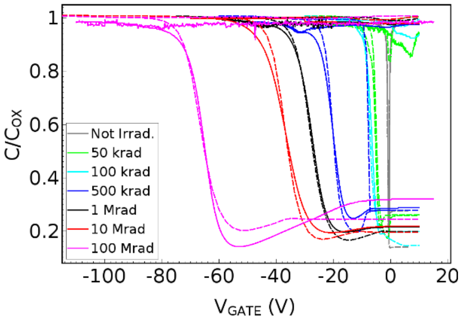

HPK MOS Capacitors

p-stop process.

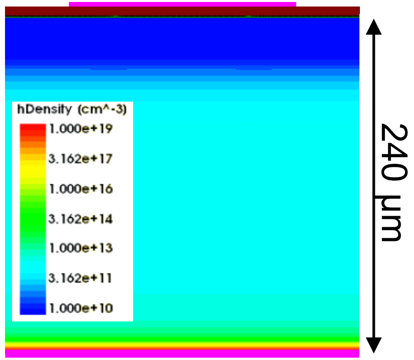

p-stop

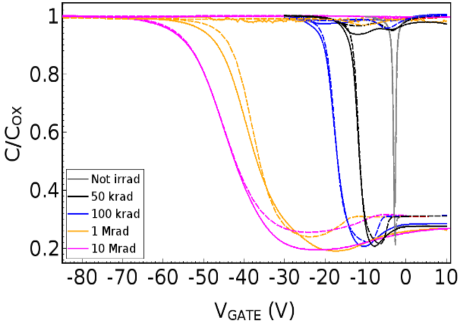

p-spray process.

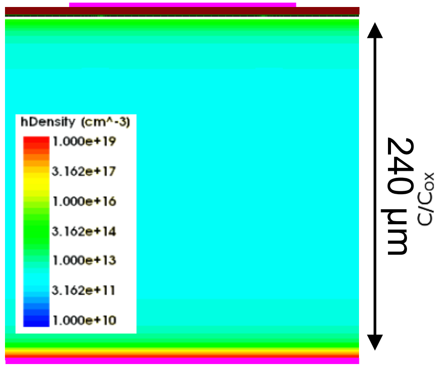

p-spray

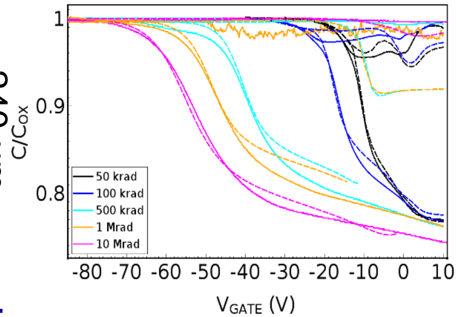

arianna.morozzi@pg.infn.it

Surface & Bulk model validation

▬▬ Measurements
– – – Simulations

HPK Gated Diodes

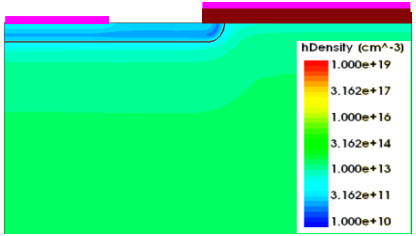

- ✓ I-V characteristics as a function of V_{GATE}.
- ✓ From I-V measurements the surface velocity s_0 was evaluated as a function of the dose.

$$s_0 = \frac{\pi}{2}\sigma_s v_{th} D_{it} k_B T \qquad s_0 = \frac{I_s}{n_i q A_G}$$

p-stop

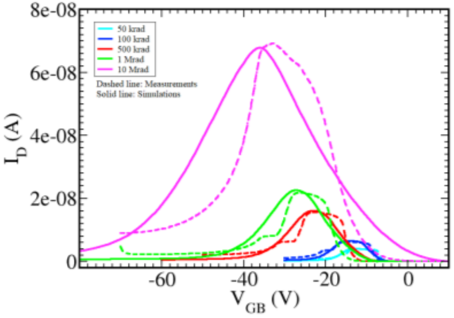

p-spray

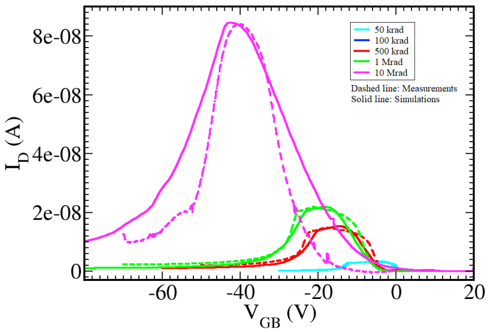

Charge Collection for silicon strips.

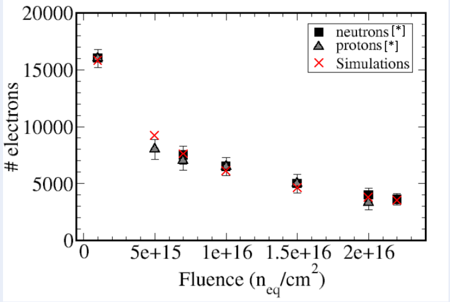

[*] A. Affolder et al., NIMA Vol. 623 (2010), pp. 177-179.

Charge Collection for PiN diodes.

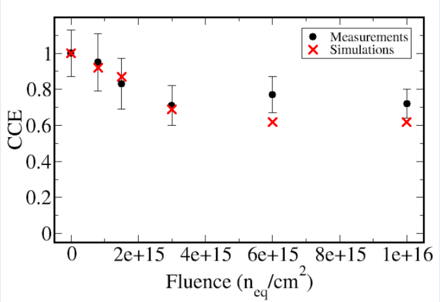

F. Moscatelli et al., IEEE TNS 64(8) (2017), pp. 2259 – 2267.
Data from M. Ferrero, 34th RD50 Workshop (2019)

arianna.morozzi@pg.infn.it

Rad-hard/Innovative materials

- ❑ Diamond
- ❑ SiC
- ❑ a:Si-H
- ❑ Ferroelectrics

CVD DIAMOND for particle detection applications

Silicon vs Diamond in **Electronics** (**radiation detection**)

	Silicon	Diamond	
Bandgap [eV]	1,12	5,47	**Higher-Field operation**
Breakdown Field [MV/cm]	0,4	20	
Intrinsic Resistivity@R.T. [Ω cm]	$2{,}3\times10^{5}$	$> 10^{11}$	**lower leakage current**
Intrinsic Carrier Density [cm^{-3}]	$1{,}5\times10^{10}$	10^{-27}	
Dielectric Constant	11,9	5,7	
Electron Mobility	1350	1900-3800	**faster signal**
Hole Mobility	480	2300-4500	
Saturation Velocity	1×10^{7}	$2{,}7\times10^{7}$	
Displacement Energy [eV/atom]	13-20	43	**radiation hardness**
Thermal Condutivity [W cm^{-1} K^{-1}]	1,5	20	**heat dissipation**
Energy to create e-h pair [eV]	3,62	11,6 - 16	
Radiation Length [cm]	9,36	12,2	
Energy Loss for MIPs [MeV/cm]	3,21	4,69	
Aver. Signal Created / 100 µm	8892	3602	**lower signal**

✓ Physically-based numerical model of Diamond

- fully implemented within the TCAD environment.
- Robust and reusable simulation framework.
- Only one fitting parameter (N_T) to reproduce the experimental behavior of diamond.
- Development of a physically based diamond numerical model (deep-level traps).
- CCE as validation figure of merit (comparison with experimental data).

CVD diamond

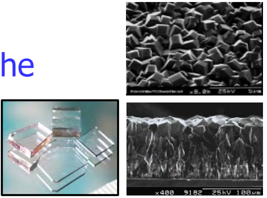

SEM images of a polycrystalline (pc) CVD diamond film: top view and cross section.

~ 12000 e/h in 150 µm

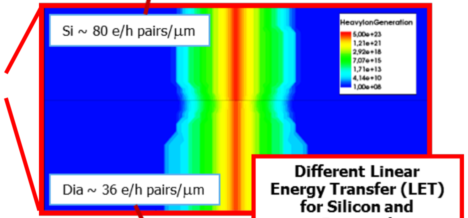

Different Linear Energy Transfer (LET) for Silicon and Diamond

~ 18000 e/h in 500 µm

Synopsys© Sentaurus TCAD

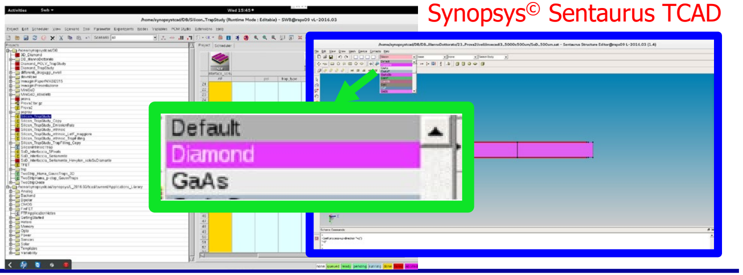

TCAD modeling of CVD DIAMOND

✓ Innovative diamond modeling for DC, TV analyses within Synopsys© Sentaurus TCAD

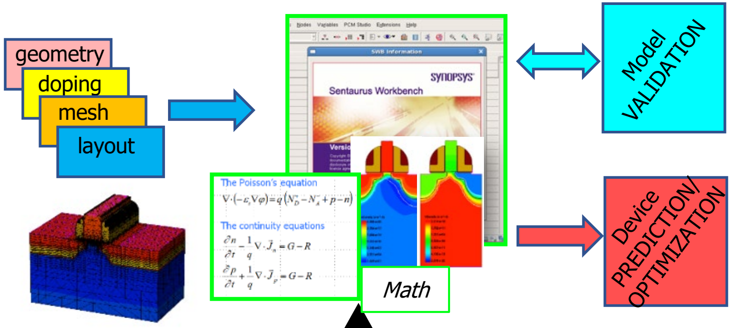

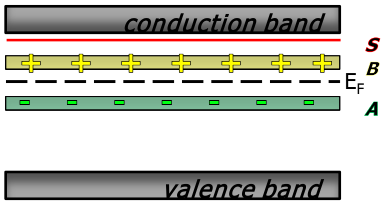

	Type	E (eV)	σ_e (cm^2)	σ_h (cm^2)	N_T (cm^{-3})
Level S	Donor	E_C - 0.05	$1\cdot10^{-13}$	$1\cdot10^{-18}$	$N_T/2$
Level B	Donor	E_C - 0.8	$1\cdot10^{-14}$	$1\cdot10^{-18}$	$N_T/2$
Level A	Acceptor	E_C - 2.7	$5\cdot10^{-16}$	$1\cdot10^{-13}$	N_T

CMOS Radiation Active Pixel Sensors (RAPS03) for particle detection

- ✓ UMC 0.18um 1P6M – no-epi layer
- ✓ Pixels (3T) with different layout options
- ✓ Thinned down to 20/25 µm

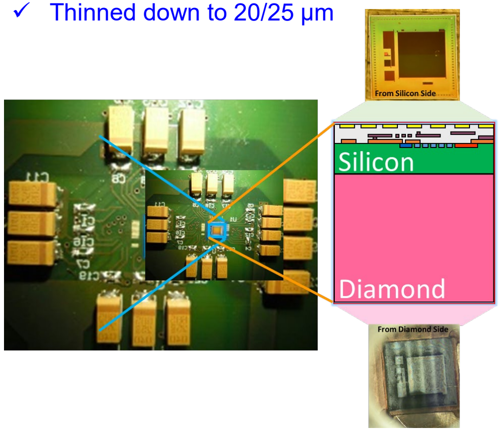

Transient Analysis

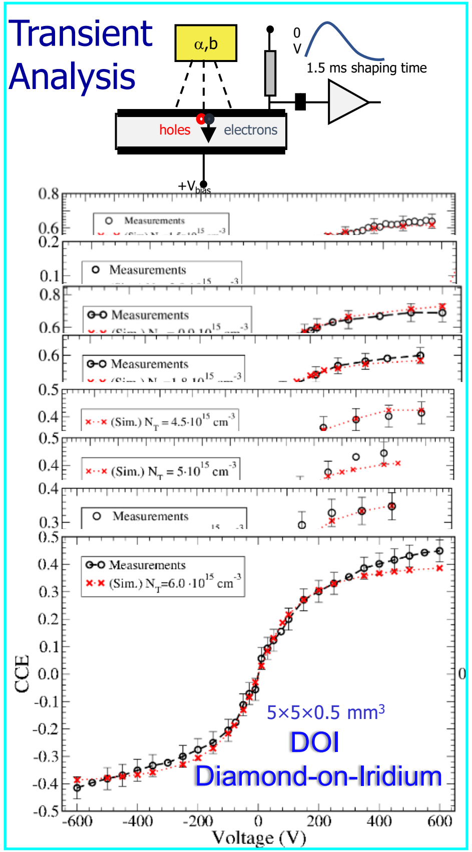

A. Morozzi et al., 13th Conference on Ph.D. Research in Microelectronics and Electronics (PRIME), pp. 73-76.
A. Morozzi et al., Materials Today: Proceedings, vol. 3, suppl. 2, 2016, pp. S153-S158, 2016.
A. Morozzi et al., JINST, 11, C12043, 2016.

arianna.morozzi@pg.infn.it

Modeling SiC devices within the TCAD environment

HEPHY
INSTITUTE OF HIGH ENERGY PHYSICS

ÖAW
AUSTRIAN ACADEMY OF SCIENCES

- ❑ 4H-SiC and 3C are already included within the standard TCAD environment.
- ❑ 4H-SiC → convergence issues
  - ❑ The wide bandgap of 4H-SiC leads to very low intrinsic charge carrier densities.
  - ❑ Usually, a much higher numeric accuracy than the default settings are required.
  - ❑ This can partially be mitigated by finer meshing.
  - ❑ Tuning error & convergence criteria and solver settings can improve convergence drastically.

Efficient meshing strategy

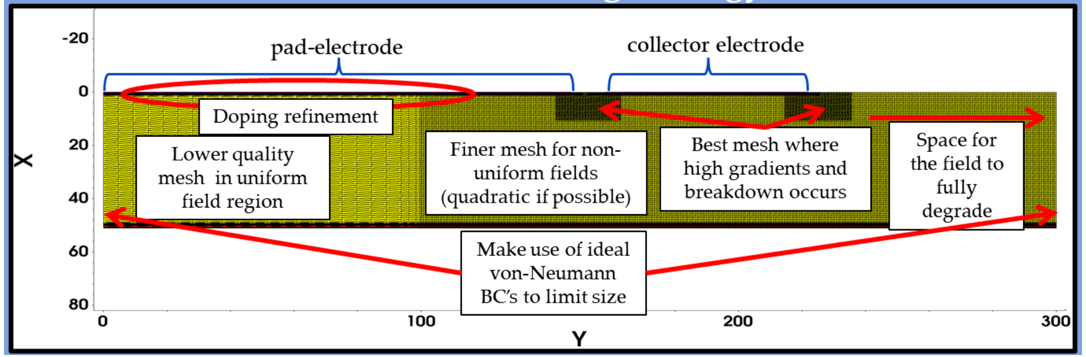

- ❑ Due to the low wafer quality (compared to Si), the Debye length is very small
- ❑ $\lambda = \sqrt{\frac{k_B T \varepsilon}{q^2 N_{Doping}}} \approx 0.3\ \mu m$

  for n-doping = 1.5·1014 cm-3
  → large

Material courtesy of T. Bergauer and Philipp Gaggl

Simulation results

- ❑ Planar 4H-SiC p-in-n diodes from CNM.
- ❑ Dominant deep level defect in 4H-SiC is $Z_{1/2}$ defect $E_T = E_C - (0.63 \div 0.71)$ eV with $N_{Z1/2} = 10^{15}$ cm^{-3} $\sigma_{Z1/2}$ = 10-15 cm^{-2}.
- ❑ Acceptor type, origin from C-Vacancy.

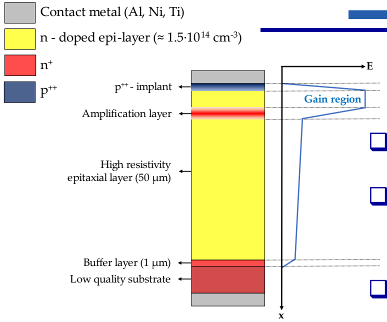

LGADs with SiC

- ❑ Design optimization.
- ❑ Additional amplification (gain) layer
- ❑ Benchmark simulations:
  - ❑ Constant epi-doping of 1.5e14 cm^{-3}
  - ❑ Gain layer doping variation

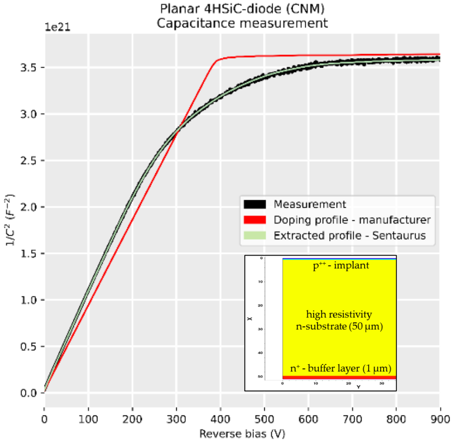

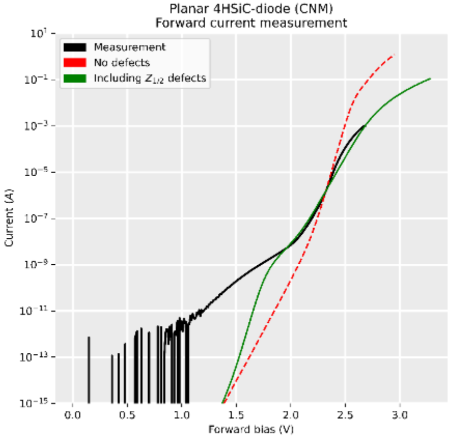

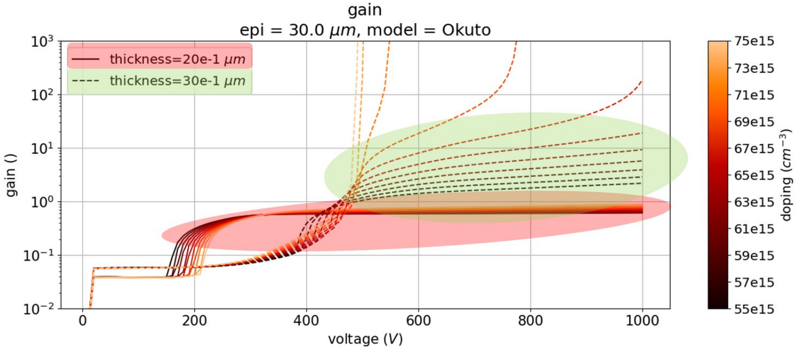

Material courtesy of T. Bergauer and Philipp Gaggl

arianna.morozzi@pg.infn.it

Hydrogenated amorphous silicon (a-Si:H)

- ☐ Proposed as a suitable material to design thin a-Si:H detectors on flexible substrates (mostly Polyimide) for beam monitoring, neutron detection, and space applications.
  - ☐ intrinsic radiation tolerance, low cost, large area (different substrates, including flexible).
- ☐ Not included within the standard Synopsys TCAD material library
  - ☐ Development of a-Si:H parametric material model.
  - ☐ Different custom mobility models have been devised and implemented within the code as external PMI (Physical Model Interfaces) and accounting for different dependencies on temperature and internal potential distribution, thus resulting in a new mobility model embedded within the code.
  - ☐ Simple test structures, featuring p-i-n diodes have been simulated and compared to experimental data as a benchmark.

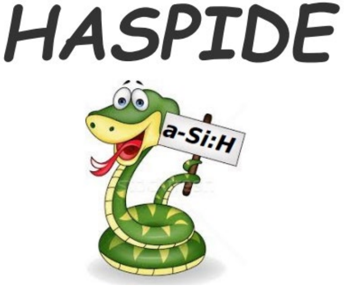

HASPIDE
and **3D-SiAm**
INFN projects

arianna.morozzi@pg.infn.it

Modeling a-Si:H devices within the TCAD environment

- ☐ Not included within the standard material library
- ☐ Parameter file developed with all the characteristics
- ☐ Traps and validation of the model

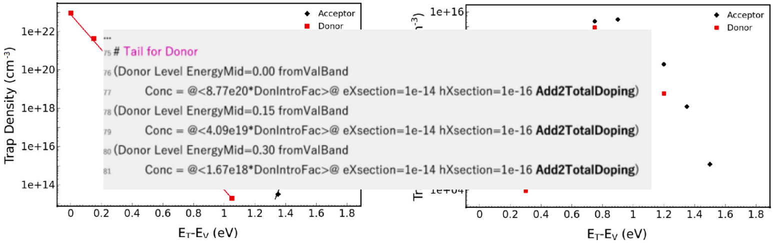

```
...
# Tail for Donor
(Donor Level EnergyMid=0.00 fromValBand
        Conc = @<8.77e20*DonIntroFac>@ eXsection=1e-14 hXsection=1e-16 Add2TotalDoping)
(Donor Level EnergyMid=0.15 fromValBand
        Conc = @<4.09e19*DonIntroFac>@ eXsection=1e-14 hXsection=1e-16 Add2TotalDoping)
(Donor Level EnergyMid=0.30 fromValBand
        Conc = @<1.67e18*DonIntroFac>@ eXsection=1e-14 hXsection=1e-16 Add2TotalDoping)
```

p-i-n device on kapton

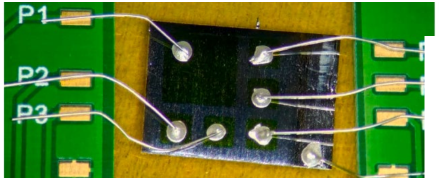

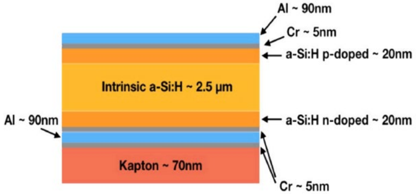

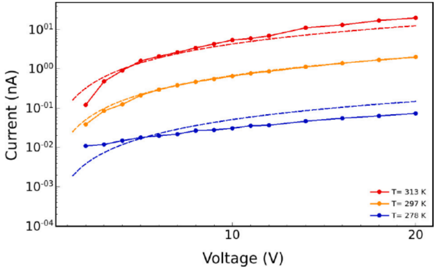

p-i-n device on crystalline Si

D. Passeri et al.

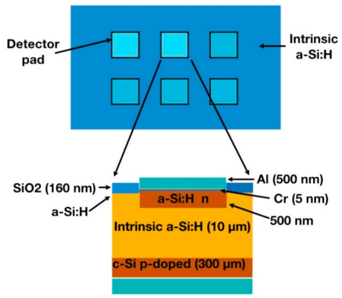

Fig. 10. p-i-n devices on crystalline silicon: simulated cross section.

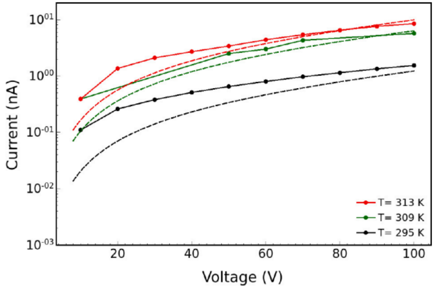

- ☐ Development of a user-defined PMI for the mobility

$$\mu = A^* V^m T^n exp\left(b\frac{\sqrt{|F|}}{T}\right)$$

HASPIDE

D. Passeri et al., Materials Science in Semiconductor Processing, 2024, 169, 107870

Negative capacitance field effect transistors for the future High Energy Physics applications

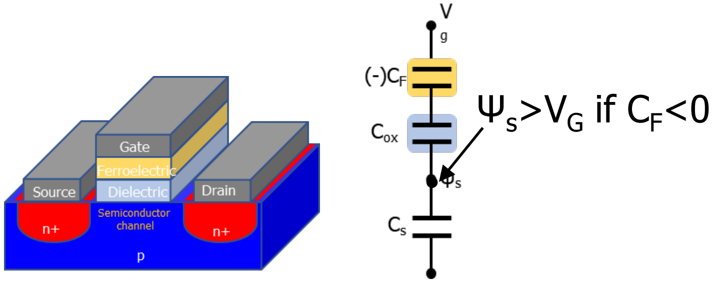

$\Psi_s > V_G$ if $C_F < 0$

Sub-threshold Swing (SS)

Body factor Transport factor

$$SS = \frac{\partial V_g}{\partial(log I_d)} = \frac{\partial V_g}{\partial \psi_s} \times \frac{\partial \psi_s}{\partial(log I_d)}$$

$$min\left(\frac{\partial \psi_s}{\partial(log I_d)}\right) = \ln(10) \times \frac{k_B T}{q} \approx 60\,\frac{mV}{decade}$$

$$\frac{\partial V_g}{\partial \psi_s} = 1 - \frac{C_s}{C_{ins}}(\alpha_f C_{ins} - 1) \quad <1$$

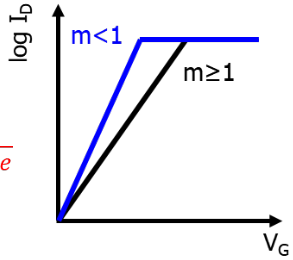

SS < 60 mV/decade typical of NC-FET

- ✓ The NegHEP project aims to investigate the radiation damage effects on Negative Capacitance Field Effect transistor
  - ✓ Issues in low signal detection in thin layers:
    - ✓ minimum detectable signal is dominated by the switching threshold of a digital switch (e.g. ≈1 ke- for 28 nm technology, <100 e- for sub 10-nm technology).
    - ✓ Continuous increase in electronics performance demand
- ✓ Proposed solution: Negative capacitance (NC) FETs
  - ✓ By replacing the standard insulator with a ferroelectric insulator of the right thickness it should be possible to implement a step-up voltage transformer that will amplify the gate voltage thus enabling low voltage/low power operation.
- ✓ Would it be possible the concept of pixelated detector with sufficiently small cells to be read out entirely by simple inverters exploiting the NC “self-amplification”?

Ferroelectric models: validation

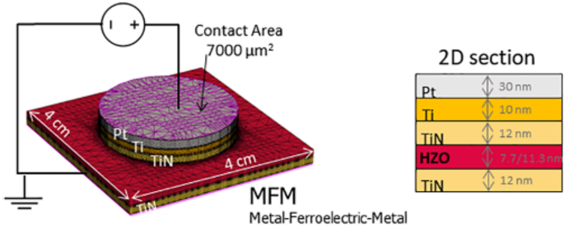

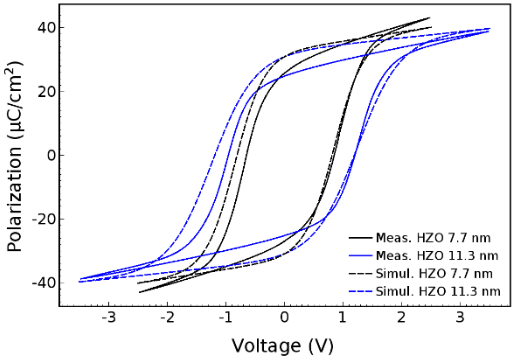

Preisach TCAD Model of hysteresis:

- ✓ remnant polarization
  Pr = 31 μC/cm^2
- ✓ saturation polarization
  Ps = 33 μC/cm^2
- ✓ coercive field
  Ec =1.1 MV/cm

for both 7.7 nm and 11.3 nm thin HZO films.

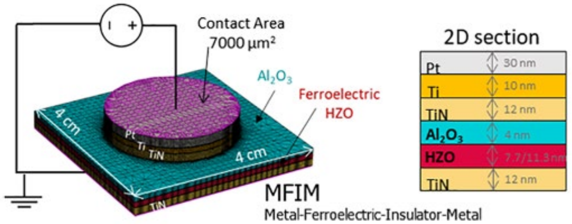

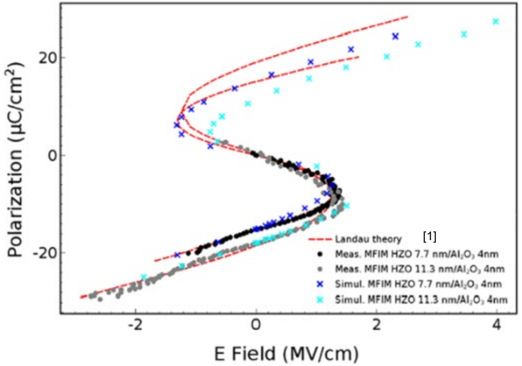

- Structures:
  - MFM (Metal-Ferroelectric-Metal)
    - tFE= 7.7 nm and 11.3 nm
  - MFIM (Metal-Ferroelectric-Insulator-Metal)
    - tFE= 7.7 nm and 11.3 nm
    - tDE = 0-4 nm

- Fabricated on Si substrates with ferroelectric $Hf_{0.5}Zr_{0.5}O_2$ (HZO) and dielectric Al_2O_3 thin films.
- The experimental setup has been implemented within the TCAD environment.
- Hysteretic P-E trend was realistically accounted for by using the TCAD Preisach model of hysteresis.
- The Landau S-shaped plot was realistically accounted for by using GLK hysteresis-free model.

A. Morozzi et al., Solid-State Electronics Volume 194, August 2022,
A. Morozzi et al 2022 JINST 17 C01048.
A. Morozzi et al., 2021 EuroSOI-ULIS), Caen, France, 2021, pp. 1-4, doi: 10.1109/EuroSOI-ULIS53016.2021.9560683.

arianna.morozzi@pg.infn.it

Ferroelectric models: application NCFETs

- ☐ Guidelines for the optimization of the NC-FETs design.
- ☐ Capacitance matching $|C_{FE}| < C_{DE}$ for the reduction of the Sub-threshold slope.

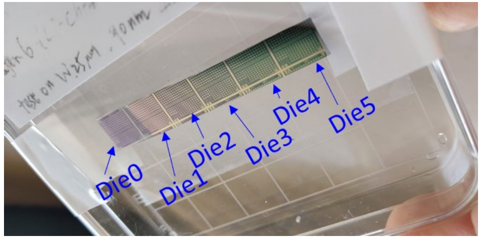

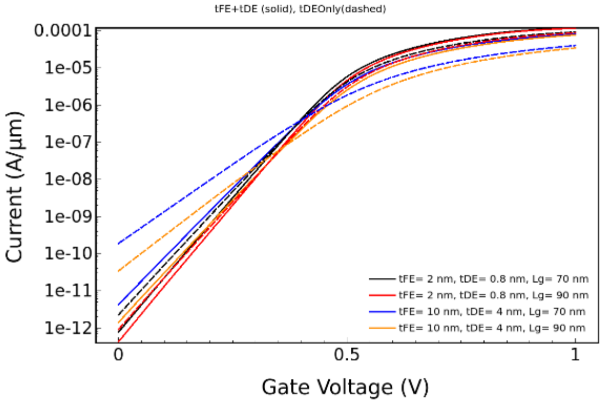
tFE+tDE (solid), tDEOnly(dashed)

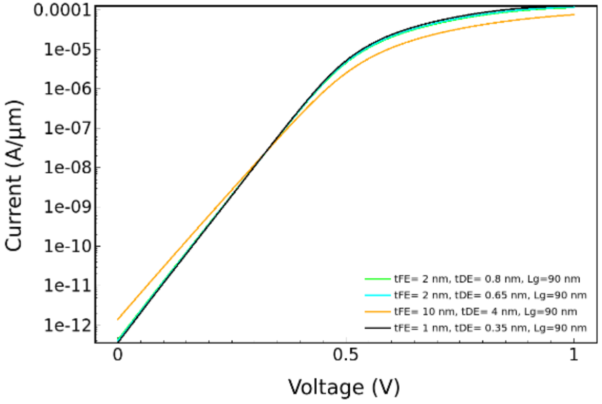

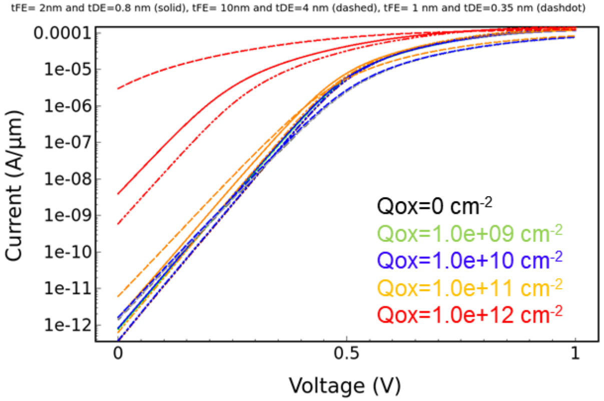
tFE= 2nm and tDE=0.8 nm (solid), tFE= 10nm and tDE=4 nm (dashed), tFE= 1 nm and tDE=0.35 nm (dashdot)

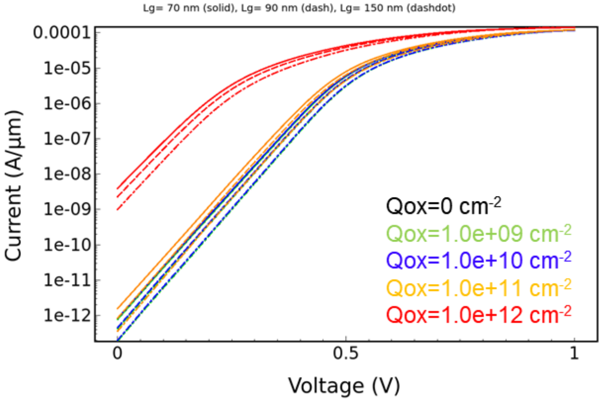
Lg= 70 nm (solid), Lg= 90 nm (dash), Lg= 150 nm (dashdot)

arianna.morozzi@pg.infn.it

Combining TCAD and Allpix Squared

- Allpix^2 is a versatile, open-source simulation framework for silicon pixel detectors.
- TCAD is crucial for understanding the fabrication process and electrical characteristics of semiconductor devices, Allpix Squared complements this by providing insights into how these devices respond to particle interactions (detailed energy deposition) and the response of pixel detectors..
- The combination of these tools enables a more holistic approach to semiconductor device design, optimization, and analysis.
- Detailed E Field maps are imported from TCAD simulations to drastically improve the precision of a sensor simulation.

Sentaurus TCAD SYNOPSYS® *Silicon to Software™*

Technology **C**omputer-**A**ided **D**esign

- ★ Model semiconductor devices by means of finite element analysis
- ★ Electric Fields: accurate and realistic

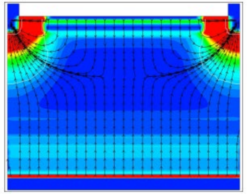

+

ap^2 allpix squared Allpix^2: Monte Carlo Simulations for Semiconductor Detectors

https://doi.org/10.1016/j.nima.2018.06.020

- ★ Simulate full response of semiconductor detector
- ★ Particle Events: fast and high statistics

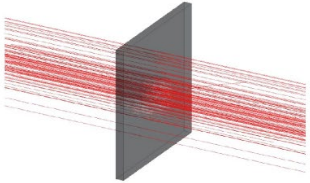

Simulation flow

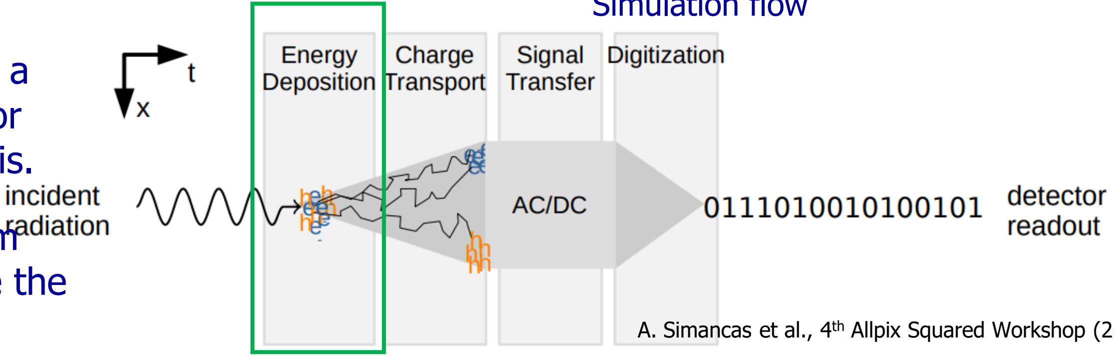

A. Simancas et al., 4th Allpix Squared Workshop (2023)

arianna.morozzi@pg.infn.it

Conclusion

- ✓ Synopsys Sentaurus TCAD powerful tool to accelerate innovation and drive the industry forward.
- ✓ Sentaurus TCAD's versatility makes it suitable for a wide range of applications.
- ✓ TCAD plays a pivotal role in the design/optimization of rad-hard devices
  - Modelling radiation damage effects is a tough task!
  - New guidelines for future production of radiation-resistant options.
  - Modeling dopant removals, impact ionization, carriers’ mobility, trap dynamics
  - Every device needs specific defect modeling (LGADs for example, prone to acceptor removal)

Thank You!